

LA-UR-

*Approved for public release;
distribution is unlimited.*

Title:

Author(s):

Submitted to:

Los Alamos

NATIONAL LABORATORY

Los Alamos National Laboratory, an affirmative action/equal opportunity employer, is operated by the University of California for the U.S. Department of Energy under contract W-7405-ENG-36. By acceptance of this article, the publisher recognizes that the U.S. Government retains a nonexclusive, royalty-free license to publish or reproduce the published form of this contribution, or to allow others to do so, for U.S. Government purposes. Los Alamos National Laboratory requests that the publisher identify this article as work performed under the auspices of the U.S. Department of Energy. Los Alamos National Laboratory strongly supports academic freedom and a researcher's right to publish; as an institution, however, the Laboratory does not endorse the viewpoint of a publication or guarantee its technical correctness.



Morphological Analyses using 3D Building Databases: Salt Lake City, Utah

Steven J. Burian and Srinivas Pradeep Velugubantla

Department of Civil Engineering

University of Arkansas

Email: sburian@engr.uark.edu; pradeep78_98@yahoo.com

Michael J. Brown

Energy and Environmental Analysis Group

Los Alamos National Laboratory

Email: mbrown@lanl.gov

LA-UR-

Los Alamos National Laboratory

October 2002

Abstract

This report summarizes our calculations of building morphological characteristics for a 6.1 km² area centered around the downtown of Salt Lake City, Utah. A three-dimensional building dataset, digital orthophotos, detailed land use/cover information, bare-earth topography, and roads were integrated and analyzed using a geographic information system (GIS). Building height characteristics (e.g., mean height, variance of height, height histograms) were determined for the entire study area and broken down by land use type using a dataset that contained 2891 buildings. Other parameters describing the urban morphology that were calculated include the building plan area fraction ($\overline{\alpha_p}$), building area density ($a_p(z)$), rooftop area density ($a_r(z)$), frontal area index ($\overline{\alpha_f}$), frontal area density ($a_f(z)$), complete aspect ratio ($\overline{\alpha_c}$), building surface area to plan area ratio ($\overline{\alpha_b}$), and the height-to-width ratio ($\overline{\alpha_h}$). Aerodynamic roughness length (z_o) and zero-plane displacement height (z_d) were calculated for the entire study area and for each land use type using standard morphometric equations and the computed urban morphological parameters.

The urban morphological parameters were computed as a function of land use type, on spatial grids, and in some cases as a function of height above ground elevation. Building statistics were correlated to underlying land use using two different land use classification schemes: the seven USGS Anderson Level 2 urban land use types and a second scheme containing more detailed residential and commercial categories. Most of the morphometric parameters that we calculated were found to be similar to values computed for other cities by other researchers. The results indicate that the calculated urban morphological parameters are significantly different between different land use types. Significant differences were also noted between subcategories of residential land use. Moreover, commercial areas were found to have very different morphological characteristics as compared to other urban land use types, primarily because commercial areas have pockets of densely packed tall buildings. The findings presented herein are intended to be utilized in urban canopy parameterizations found in mesoscale meteorological and urban dispersions models.

1.0 Introduction

Describing the urban terrain and land use/land cover (LULC) characteristics accurately is vital for urban planning, environmental management, environmental modeling, and many other applications. Urban terrain elements can be broadly classified as natural landscape, ornamental vegetation, bare soil or rock, buildings, impervious surfaces, driveways, sidewalks, or other infrastructure. Comprehensive urban databases containing urban terrain and LULC information are essential inputs for numerous meteorological modeling applications, e.g., simulating the atmospheric flow over cities, quantifying energy fluxes radiated to and from urban surfaces, determining the fate and transport of atmospheric contaminants in built-up areas. The minimum datasets required to describe the urban terrain in three dimensions include bare-earth digital elevation model (DEM), tree canopy and vegetative cover, land use/land cover, infrastructure, and building footprint outlines with height attribute.

The motivation for this research is the need to efficiently compute building morphological parameters for mesoscale meteorological modeling and air quality applications (see Ratti et al. 2001 and Brown 1999). The research objectives are to collect detailed urban datasets in a geographic information system (GIS) environment, develop automated procedures to calculate building morphological parameters, and integrate these urban canopy parameter values with detailed LULC datasets to derive relationships between the parameters and urban land use type. This report describes our efforts for a 6.1-km² section centered on the downtown of Salt Lake City, Utah. In the next section of this report a brief accounting of prior efforts in this area is given, followed by a description of the accumulated datasets in the Salt Lake City GIS database in Section 3.0. In Section 4.0, we include an overview of how the building morphological parameters are used in the models, a short description of the calculation procedures for deriving the morphological parameters, and then present the calculation results. The report ends with a summary in Section 5.0.

2.0 Background

A handful of researchers over the years have pioneered the work on obtaining building morphological statistics for cities (e.g., Ellefsen 1990, Voogt and Oke 1997, Cionco and Ellefsen 1998, Grimmond and Oke 1999). These studies have provided much useful information on building parameters, focusing mostly on residential areas and, for a few cities, industrial and commercial areas as well. There are not enough analyses, however, to make generalizations about building statistics for all U.S. cities. In addition, many of the analyses did not include the full complement of building statistics required by the CBNP suite of atmospheric transport and dispersion models. Past work involved detailed *in situ* studies, using visual surveys of buildings in an area encompassing a few city blocks and extrapolating the results to the entire city. With the recent availability of digital 3D building data sets, calculation of building statistics has become automated using image analysis and geographical information system (GIS) software allowing larger areas to be analyzed (e.g., Ratti et al., 2001; Burian et al., 2002a). We have recently completed a data report on building morphological statistics for downtown Los Angeles (Burian et al., 2002b), and have been working on analyses for Portland, Albuquerque, Phoenix, Oklahoma City, and Houston. Eastern U.S. cities will be addressed in future studies.

3.0 Salt Lake City Urban Database

3.1 Urban Morphology

Urban building, tree canopy, and DEM datasets can be purchased from commercial vendors or derived in-house. The resolution, accuracy, cost, and level of detail are important dataset characteristics to consider during the acquisition phase. The basic level of information supplied with purchased building datasets is typically the building footprint and the elevation of the rooftop. More sophisticated (and likely more expensive) datasets will have greater detail of the building (e.g., representation of rooftop structures) and include additional pieces of information (e.g., rooftop color and pitch, materials). Table 1 lists several commercial vendors that provide building, tree canopy, and DEM datasets and other digital urban data products. Digital building datasets can currently be obtained for numerous U.S. and international cities and more are rapidly becoming available. In most cases the vendor can provide the dataset in a variety of generic vector or raster data formats or data formats specific to the commercial software packages (e.g., ESRI shapefiles).

Table 1. Commercial vendors of building datasets

Vendor	Web Site
i-cubed	www.i3.com
Istar USA	www.istar.com
The Gemi Store	www.gemistore.com
Urban Data Solutions, Inc.	www.u-data.com
Vexcel Corporation	www.vexcel.com
Terrapoint (lidar)	www.transamerica.com/business_services/real_estate/terrapoint/default.asp

We contracted Urban Data Solutions, Inc. (UDS) to prepare the high-resolution building dataset of the Salt Lake City (SLC) downtown area in both vector/raster GIS forms and detailed AutoCAD format. The CAD-formatted drawings are very detailed showing complex multi-level building information and details of rooftop structures. The GIS shapefile-format building data are simpler, containing building footprints with rooftop elevation as an attribute, as well as other information about the rooftops (e.g., pitch, color). In the GIS dataset, the buildings are represented as 2D polygons and in the AutoCAD drawing the buildings are composed of a mixture of 3D faces and 2D polylines. For both data formats the planimetric (x,y) accuracy is 2 meters and vertical (z) accuracy is 2.5 meters. The ESRI shapefile is composed of geometric information, attribute information, and topology. A major limitation of the shapefile dataset compared to the CAD dataset is its lack of representation of non-horizontal surfaces. For example, pitched rooftops must be approximated as a series of horizontal polygons in the GIS dataset (if defined at all), but can be accurately defined in 3 dimensions in CAD. The primary limitation of the CAD dataset is the inability to numerically process the information to compute the building morphological parameters. The Salt Lake City building dataset includes 2,891 buildings and covers an area of 6.1 km² that encompasses the downtown region and adjacent areas of predominantly residential, industrial, and commercial land uses (see Figures 1 and 2).

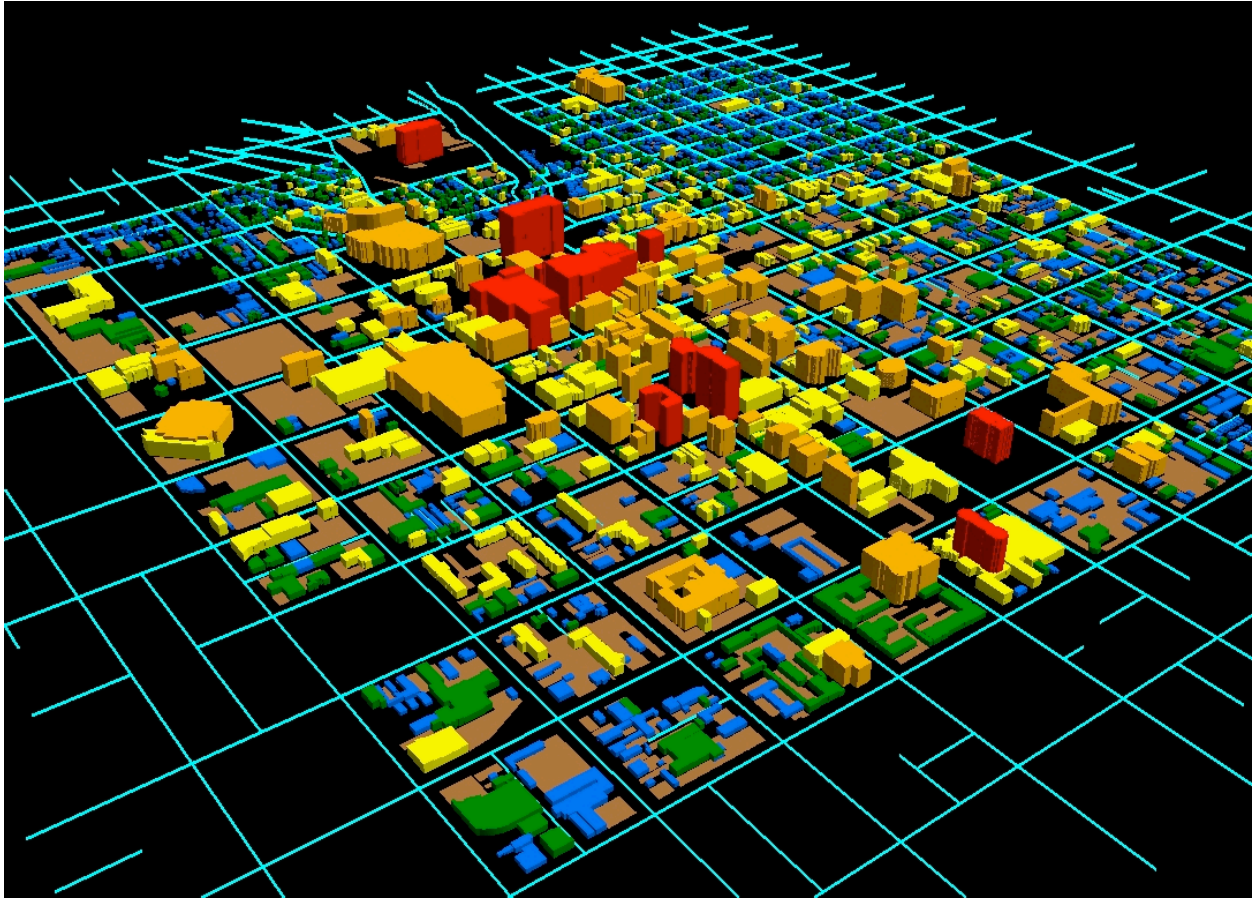


Figure 1. 3-D view from the southwest of the Salt Lake City building database. The domain covers a 6.1-km² area. Buildings are overlaid onto a street map with paved parking areas shown in brown.

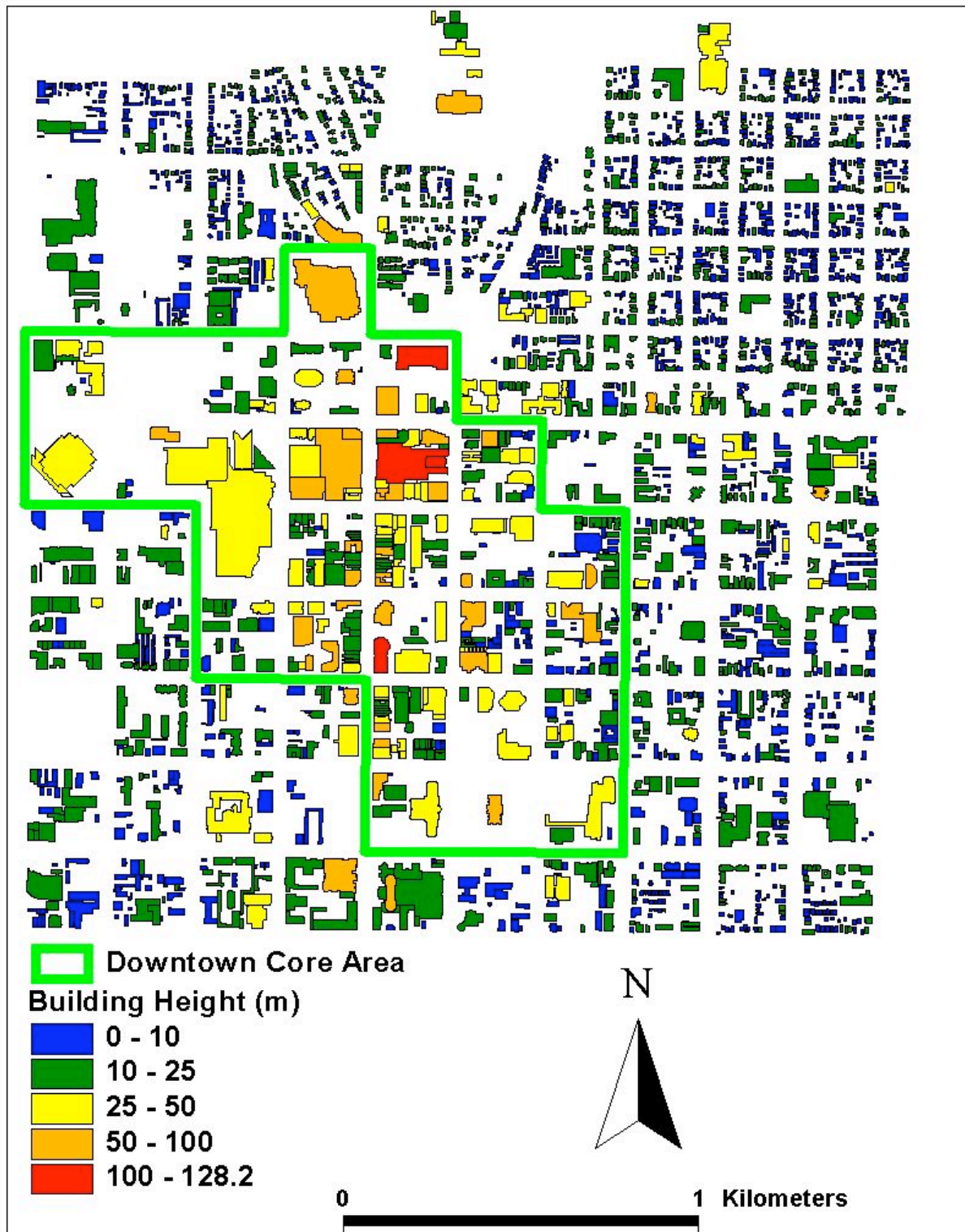


Figure 2. Plan view of the Salt Lake City building database. The domain covers 6.1 km². Buildings are color-coded by height.

3.2 Urban Land Use/Land Cover (LULC)

A major objective of this research project is to derive relationships between building morphological parameters and urban land use type. To meet this objective we need to spatially relate building morphological parameters with a manageable number of urban land use types. LULC data for areas in the United States can be obtained from several sources including federal agencies (e.g., U.S. Geological Survey (USGS), U.S. Environmental Protection Agency (USEPA)), state agencies, local/regional planning agencies, universities, researchers, commercial vendors, and others. In general, datasets obtained from the federal, state, local/regional planning agencies, universities, or other researchers are free or cost a nominal fee. Commercial vendors on the other hand will provide a specific product with additional quality control for a greater price.

Three existing LULC datasets were obtained for Salt Lake City and evaluated for use in this study. The USGS/EPA GIRAS dataset was unacceptable for this study because it was not representative of current urban land use as determined by viewing a year 2000 high-resolution (6-inch pixel resolution) digital orthophoto overlaid with the dataset. Areas of residential and commercial land use shown in the digital orthophoto were not represented as urban land use in the USGS dataset. The second dataset evaluated was the National Land Cover Dataset (NLCD), which was also found to be unacceptable because it did not have a sufficient number of urban land use categories. On the positive side, the NLCD does distinguish between high and low intensity residential, but it does not distinguish commercial from industrial from transportation. This distinction is critical because building morphological parameters are significantly different between commercial and industrial land uses. The final LULC dataset evaluated was from the State of Utah Water Resources Division (UWRD). Once again, this dataset was unacceptable because it did not have a sufficient number of urban land use categories. Therefore, unable to find an existing dataset to meet our needs we chose to modify the UWRD dataset by re-classifying parts of the study area manually using the high-resolution digital orthophoto. Specifically, we revised the UWRD land use dataset by observing the orthophoto block by block and adjusting the data where discrepancies between the dataset and the orthophoto were noticed or where a more detailed land use classification could be made.

The final LULC coverage for the Salt Lake City area had two urban land use classification schemes: the first corresponding to the USGS Anderson Level 2 categories and the second with more detailed classification of the Residential, Commercial & Services, and Other Urban or Built-up land use categories. This land use classification is consistent with previous building morphological work completed for Los Angeles (Burian et al. 2002b). Table 2 summarizes the land use types in each classification scheme and Appendix 1 provides further descriptions of the land use categories. The seven categories for the first scheme are (1) Residential, (2) Commercial & Services, (3) Industrial, (4) Transportation/Communications/Utilities, (5) Mixed Industrial & Commercial, (6) Mixed Urban or Built-up, and (7) Other Urban or Built-up. This is the same scheme used to classify urban land use in the USGS/EPA GIRAS national LULC dataset. The second classification scheme contains subcategories for Residential, Commercial & Services, and Other Urban or Built-up land use types. The Residential category is divided into four subcategories: (1) Low-density Single-family, (2) High-density Single-family, (3) Multifamily, and (4) Mixed. Building density and vegetation characteristics are expected to be

significantly different between the four types of residential land use. The Commercial & Services category is divided into two subcategories: Non-high-rise and High-rise. The rule used to differentiate between Non-high-rise and High-rise was based on fraction of buildings in a city block with heights 17.5 m or greater (corresponding to approximately 5 stories or greater). If more than 20% of the buildings in a Commercial & Services land parcel were 17.5 m or greater the parcel was classified as High-rise, otherwise it was classified as Non-high-rise. The Other Urban or Built-up category is also divided into two subcategories: Predominantly Vegetated and Predominantly Built-up.

Another land use category called Urban High-rise was defined in order to analyze and define the characteristics of high-rise areas throughout the entire city, not just those in the Commercial & Services land use category. Urban High-rise was defined according to the rules used to differentiate the Commercial & Services land use into High-rise and Non-high-rise (greater than 20% of the buildings per parcel with heights of 17.5 m or greater). In addition, a Downtown Core Area was delineated to include the city center according to our collective opinion formed by knowledge of the city, site visits, and the digital orthophoto. These two newly-defined classes will overlap with the land uses in our two classification schemes, but are needed so we can analyze and better define the characteristics of high rise and city center areas of cities.

Our land use data indicates that the 6.1-km² study area is a highly urbanized region of Salt Lake City consisting of a part of the downtown region (containing high-rise buildings), as well as High-density Single-family Residential and Industrial areas. The land use distribution listed in Table 2 suggests that most of the land use is Commercial & Services and Residential with a small fraction of Industrial and Mixed Urban or Built-up. This land use distribution is similar to other cities we have analyzed (e.g., Burian et al. 2002b).

Note that Low-density Single-family Residential is not present in the study area. Low-density, in this study, is defined as Residential land use containing on average less than 8 detached single-family housing units per hectare, while high-density is defined as Residential land use with higher housing unit density. The 8 housing units per hectare corresponds to approximately a $\frac{1}{4}$ -acre lot size, effectively dividing the $\frac{1}{4}$ -acre size lots common for medium- to high-density developments in the U.S., from the lower density $\frac{1}{2}$ -acre and larger lot sizes. Although the study area in Salt Lake City does not contain Low-density Single-family Residential land use, the classifications used in this study will be used for analyses of other cities and other parts of Salt Lake City where low-density residential is present.

Figure 3 shows our derived LULC dataset for the 6.1-km² study area in Salt lake City after aggregation to the 12-category land use scheme. Also shown is the boundary of the Downtown Core Area. The LULC dataset was intersected with the building dataset using the ESRI ArcView GIS software to identify which buildings were associated with which land use type. Fortran codes and Avenue scripts previously written, as well as standard ArcView GIS functions, were used to calculate a suite of urban morphological parameters. The calculation procedures and the results of the analyses are described next in Section 4.

Table 2. Urban land use coverage in the 6.1-km² study area

Land Use Class	Area (ha)*	Percent of Total (%)
Residential	159	26
Low-density Single-family (< 8 units/hectare)	0	0
High-density Single-family (≥ 8 units/hectare)	47	8
Multifamily	36	6
Mixed	76	13
Commercial & Services	336	55
Non-high-rise	137	22
High-rise	199	33
Industrial	47	8
Transportation/Communications/Utilities	0	0
Mixed Industrial & Commercial	0	0
Mixed Urban or Built-up	44	7
Other Urban or Built-up	22	4
Predominantly Vegetated	4	<1
Predominantly Built-up	19	3
Urban High-rise	202	33
Downtown Core Area	163	27

* The areas are given in hectares (ha) (100 ha = 1 km²).

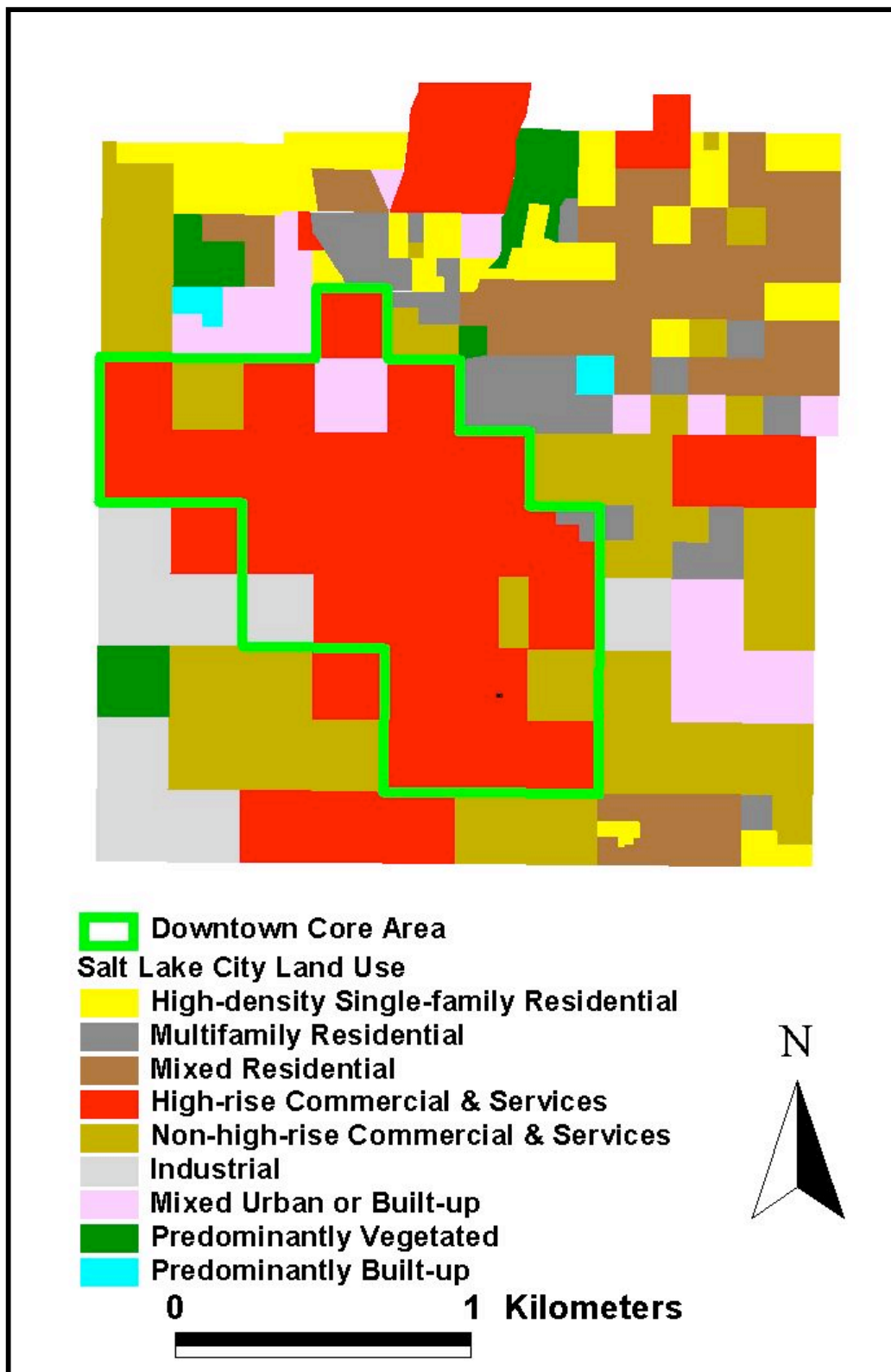


Figure 3. LULC dataset for the 6.1-km² study area aggregated to 12-category building analysis land use classification scheme.

4.0 Derivation of Urban Morphological Parameters

In the next ten sub-sections, we calculate building morphological parameters that are used in atmospheric models and dispersion model to account for urban effects. These calculations include building height statistics, the building plan area fraction (\bar{f}_p), building area density ($a_p(z)$), rooftop area density ($a_r(z)$), frontal area index (\bar{f}_F), frontal area density ($a_F(z)$), complete aspect ratio (\bar{f}_C), building surface area to plan area ratio (\bar{f}_B), height-to-width ratio (\bar{f}_S), the roughness length (z_o), and the displacement height (z_d). The calculation procedures and results are summarized in each sub-section.

4.1 Building Height Characteristics

Background. In this sub-section we summarize the height characteristics of buildings in the 6.1-km² study area. Average building height yields information on the depth through which the urban canopy directly impacts the atmosphere. Average building height (multiplied by a proportionality constant) can be used as a first-order approximation of the surface roughness z_0 (see Section 4.10). Surface roughness is used in air quality and meteorological models to account for enhanced mixing and the drag effects of the underlying surface. Canopy height is often used as the length scale in the canopy layer. Urban field experiment data evaluations have suggested that similarity theory is valid somewhere above the canopy height. Below canopy height, drag parameterizations can be used to account for reduced air flow due to the urban fabric. Variation in canopy height may prove to be important in parameterizations of turbulence production.

Calculation Methods. The mean and standard deviation of building height were calculated using the following equations:

$$\bar{h} = \frac{\sum_{i=1}^N h_i}{N} \quad (1)$$

$$s_h = \sqrt{\frac{\sum_{i=1}^N (h_i - \bar{h})^2}{N - 1}} \quad (2)$$

where \bar{h} is the mean building height, s_h is the standard deviation of building height, h_i is the height of building i , and N is the total number of buildings in the area. The average building height weighted by building plan area was calculated using the following equation:

$$\bar{h}_{AW} = \frac{\sum_{i=1}^N A_i h_i}{\sum_{i=1}^N A_i} \quad (3)$$

where \bar{h}_{AW} is the mean building height weighted by building plan area, and A_i is the plan area at ground level of building i .

Results. For the 6.1-km² study area, the mean building height based on Eqn. (1) was calculated to be 12.1 m and the standard deviation was calculated to be 10.2 m. The mean building height weighted by plan area was computed to be 25.5 m for the study area, indicating that taller buildings have greater plan area on average. The building heights in the study area range from 1.5 m to 128 m.

Figure 4 is a histogram of building heights for the study area. Note that the building height bin widths are not equal and grow in size with height. The distribution is unimodal, with nearly 80% of the buildings being between 5 and 15 m high. More than 50% of the buildings in the study area have heights of 10 meters or less. There are only 4 buildings with heights greater than 100 meters. Interestingly, only 6% of the buildings have heights less than 5 m. As noted in Section 3, the study area is predominantly Commercial & Services and High-density Single-family Residential land use. Site visits and observation of the orthophoto indicated that the High-density Single-family residential land use areas contain mostly 2-3 story structures, which helps to explain the lack of single-story structures.

Figures 5, 6, 7, 8, and 9 show the building height histograms for five of the land uses in the 7-category land use scheme: Residential, Commercial & Services, Industrial, Mixed Urban or Built-up, and Other Urban or Built-up. Figures 5 and 7 show that Residential and Industrial buildings are predominantly two or three story structures, with a few high-rise apartment buildings present in the residential area. In the Commercial & Services land use category (Fig. 6) we observe a higher frequency of buildings with heights greater than 25 meters as compared to the other land uses, which is expected because it includes the downtown area with high rises. The building height distributions for the Residential (Fig. 5), Industrial (Fig. 7), Mixed Urban or Built-up (Fig. 8), and Other Urban or Built-up (Fig. 9) land use types have similar building height distributions with a 5-10 m mode and greater than 75% of the buildings between 5 and 15 m tall.

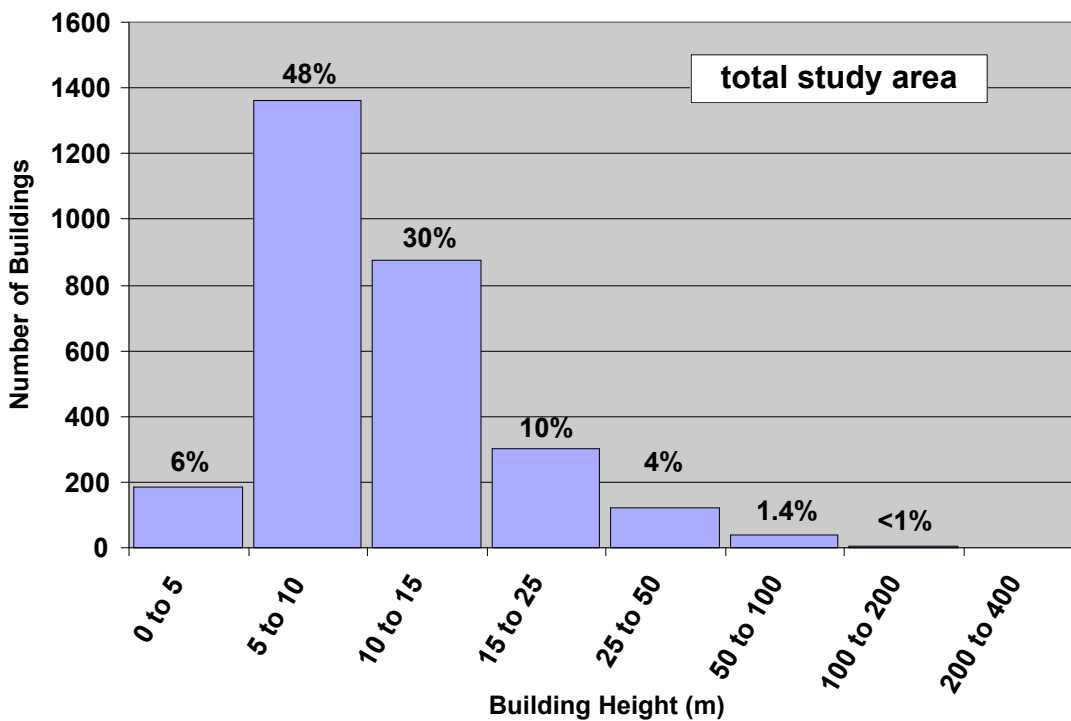


Figure 4. Distribution of building heights in the 6.1-km² downtown Salt Lake City study area. The percent of buildings in each height category are shown above each bar in the chart.

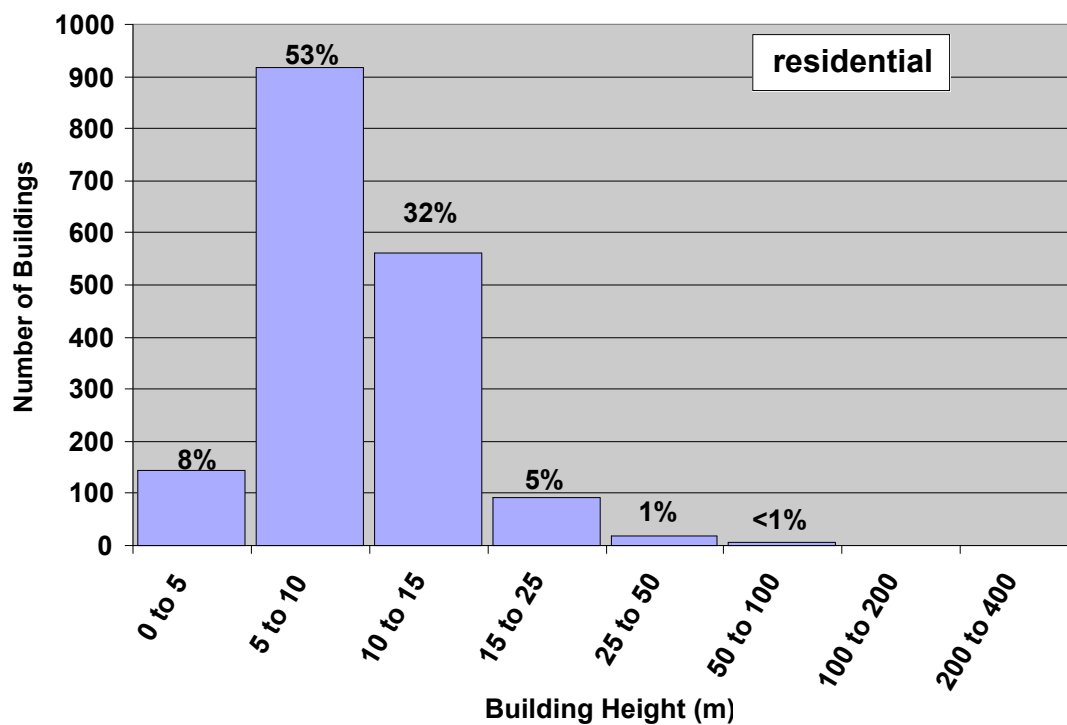


Figure 5. Distribution of building heights in the Residential land use category.

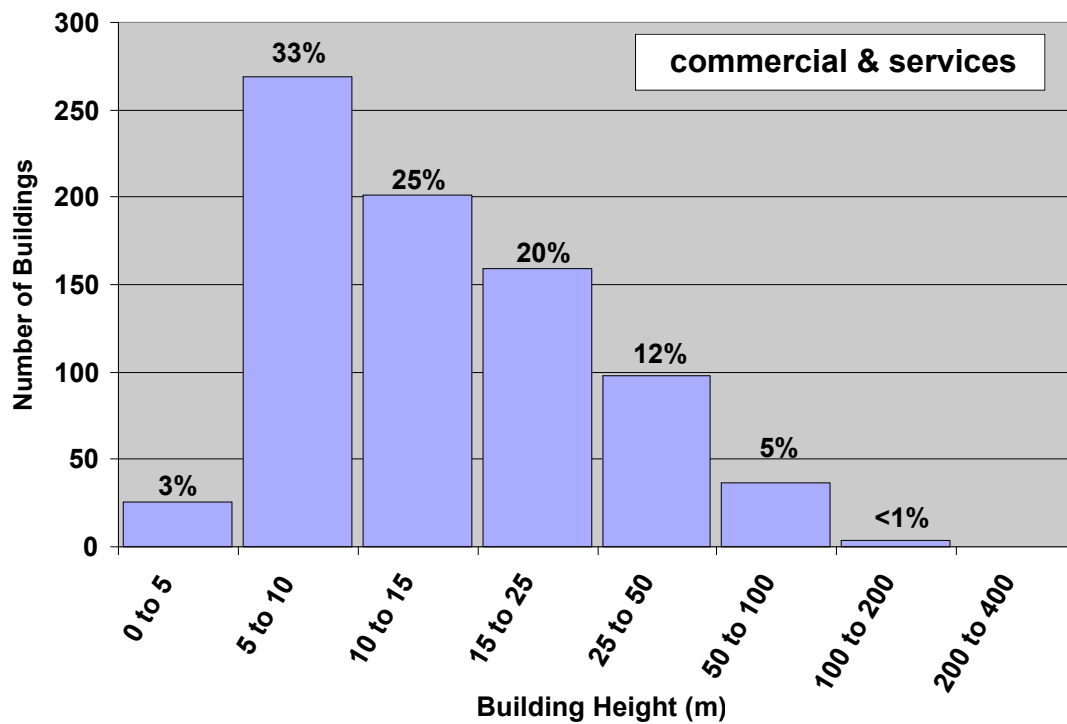


Figure 6. Distribution of building heights in the Commercial & Services land use category.

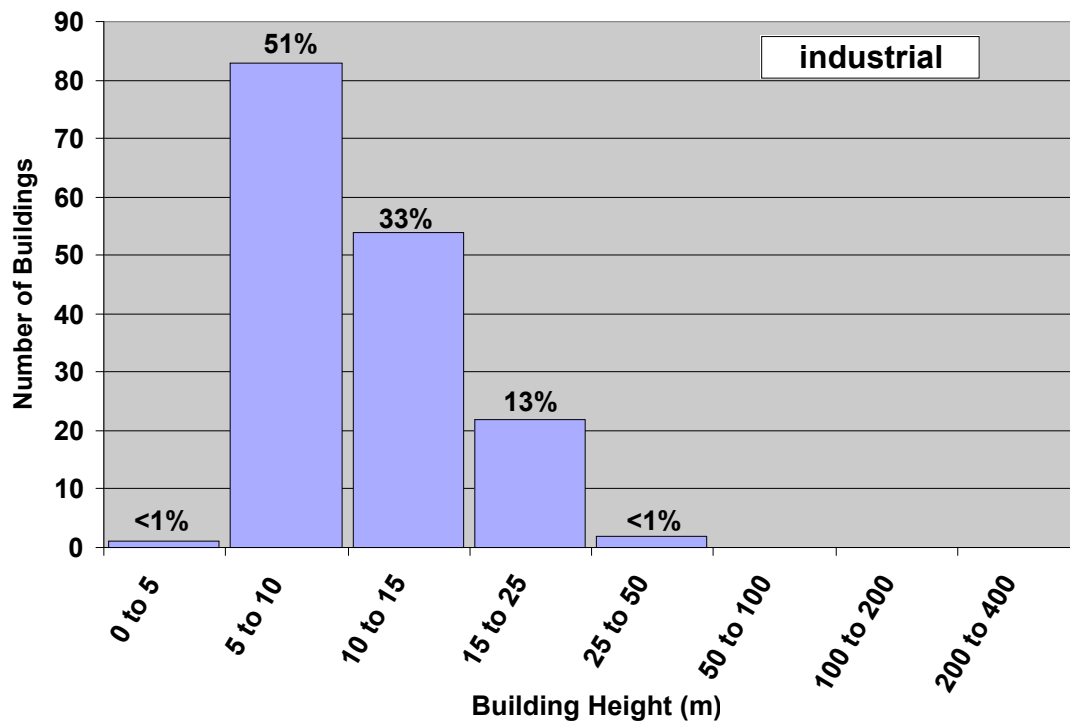


Figure 7. Distribution of building heights in the Industrial land use category.

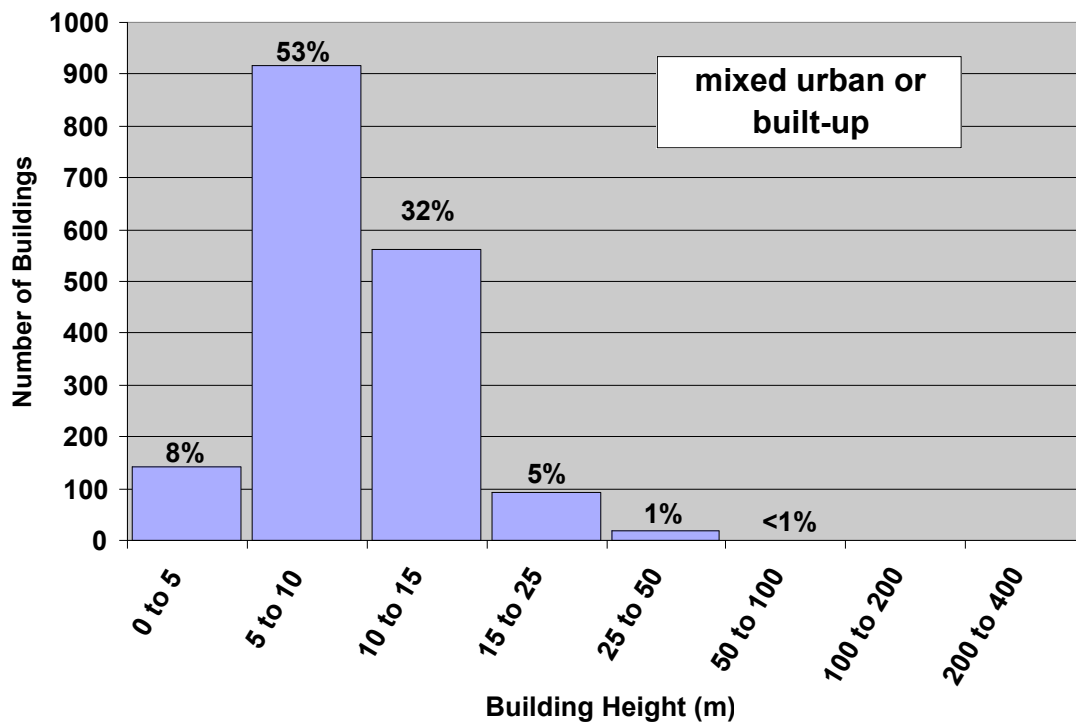


Figure 8. Distribution of building heights in the Mixed Urban or Built-up land use category.

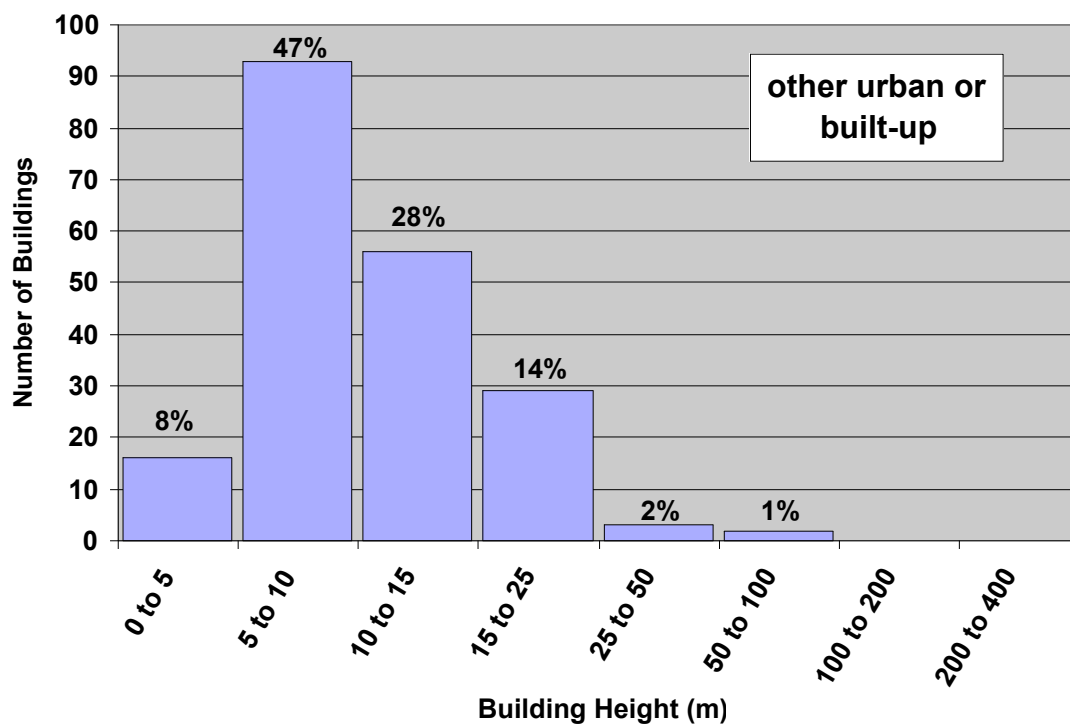


Figure 9. Distribution of building heights in the Other Urban or Built-up land use category.

Figures 10, 11, and 12 show the building height histograms for three of the four subcategories of Residential land use contained in the Salt Lake City dataset (recall that Low-density Single-family Residential land use is not found in the study area). The High-density Single-family Residential land use category has the same building height distribution as the Mixed Residential land use category (compare Figs. 10 and 12). The Multifamily Residential land use category contains high-rise apartment and condominium buildings; therefore, the building height distribution contains a higher frequency of buildings in the 10-15 and 15-25 meter height bins (Fig. 11).

Figures 13 and 14 show the building height histograms for the two subcategories of Commercial & Services land use: High-rise and Non-high rise. Clearly the Commercial & Services High-rise land use contains predominantly taller buildings, especially in the 25-50 m range. The buildings in the Commercial & Services Non-high-rise land use category are mostly shorter than 25 m. These results indicate that a sub-division of the Commercial & Services land use category into two sub-categories, if possible, would be useful for atmospheric transport and dispersion modeling applications.

Figures 15 and 16 show the building height histograms for the Urban High-rise and the Downtown Core Area land use categories. The Urban High-rise and Downtown Core Area have very similar building height distributions. Both have a uniform distribution of buildings in the 5-10, 10-15, 15-25, and 25-50 height bins, with a small percent of buildings less than 5 m and greater than 50 m. This can partially be explained because the Urban High-rise category contains the entire Downtown Core Area.

Figure 17 displays a comparison of building height histograms in percentage form for all land use types in the 7-category classification scheme all in the same plot. Figure 18 shows the height histogram comparison for the 12-category land use scheme (the plot only includes those land use present and containing a significant number of buildings) and the Urban High-rise and Downtown Core Area land uses. One can better see in these plots the similarities (e.g., similarity between High-density Single-family Residential and Mixed Residential) and differences between different land use categories. Recall, however, that some of the land uses have significantly more buildings than others.

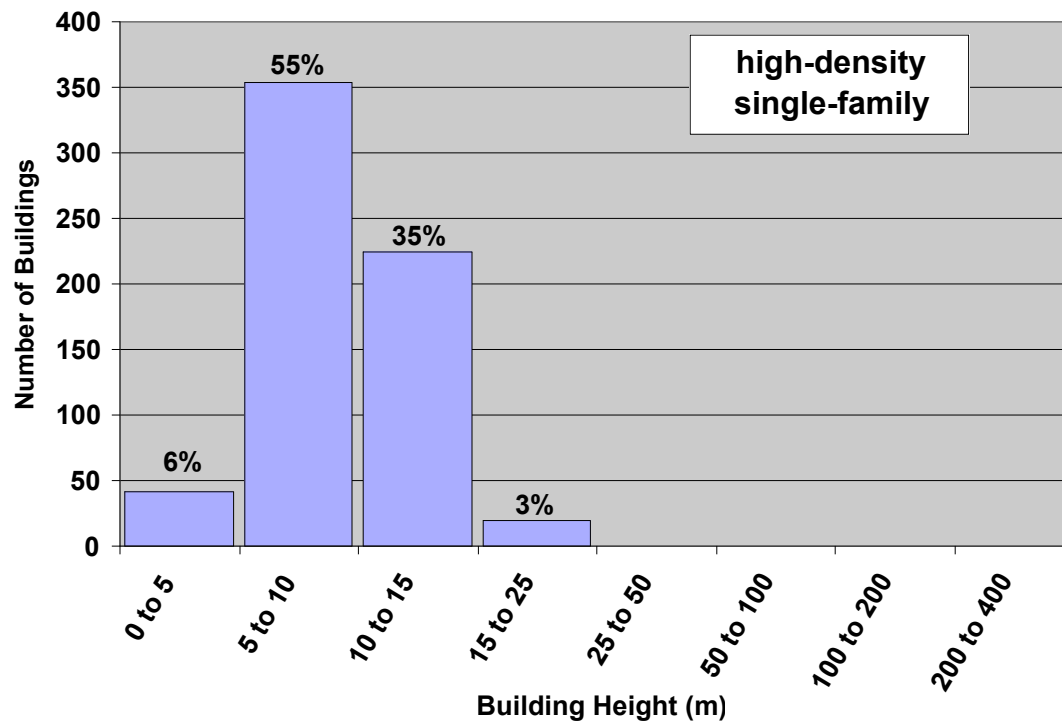


Figure 10. Distribution of building heights in the High-density Single-family Residential land use category.

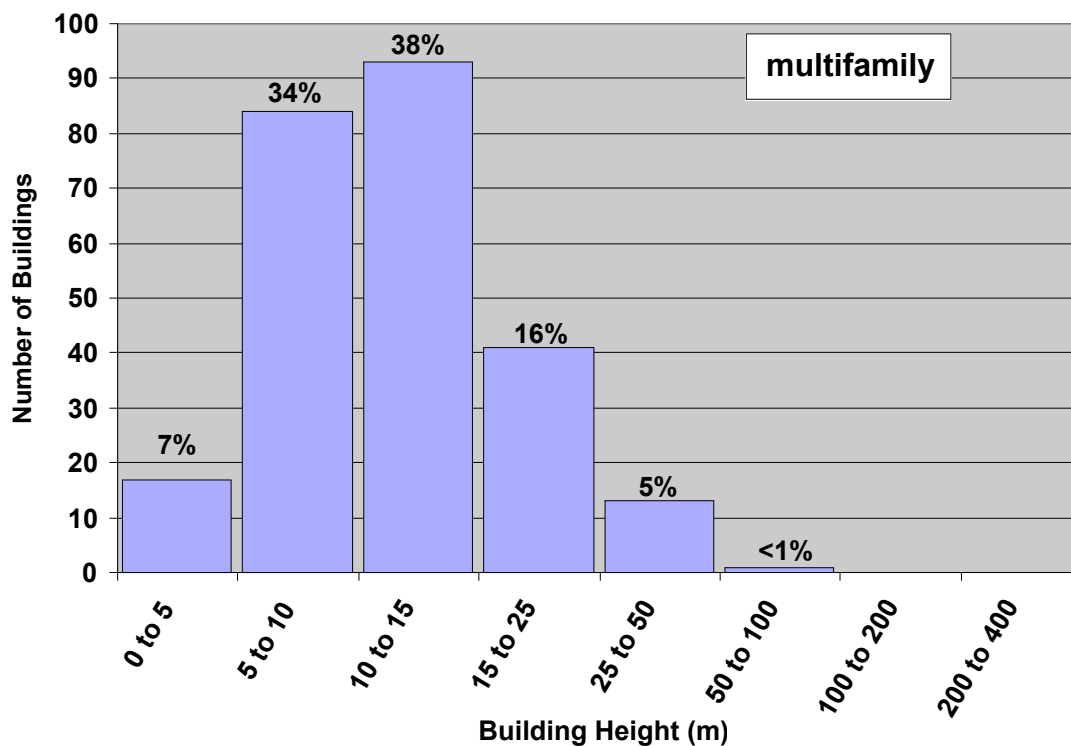


Figure 11. Distribution of building heights in the Multifamily Residential land use category.

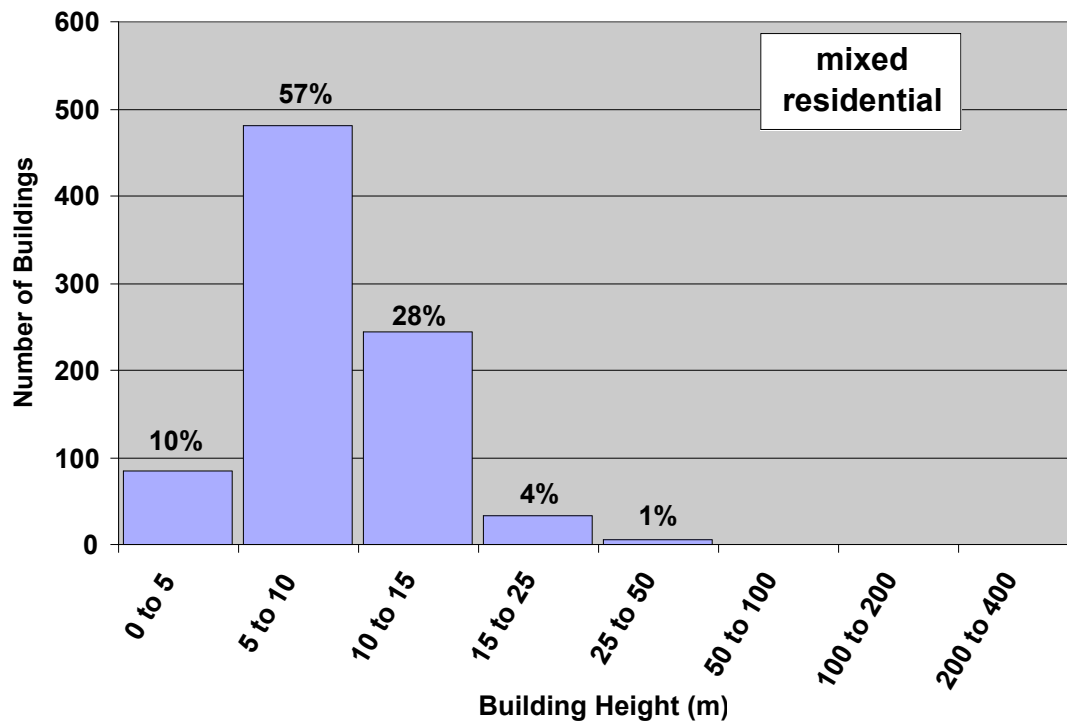


Figure 12. Distribution of building heights in the Mixed Residential land use category.

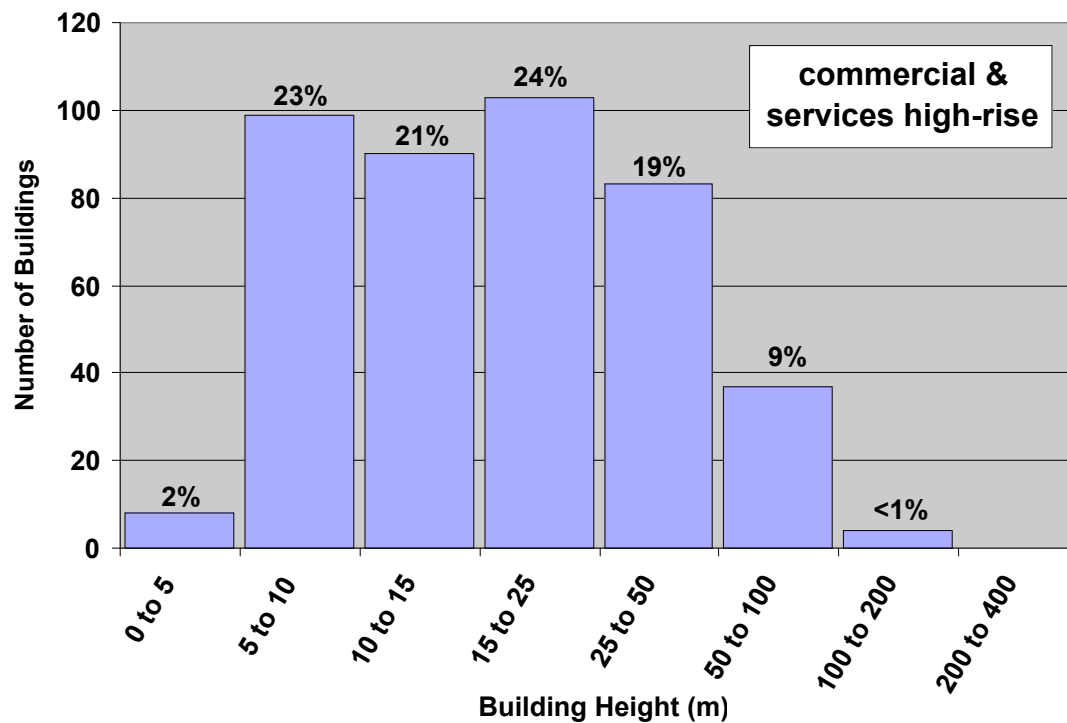


Figure 13. Distribution of building heights in the Commercial & Services High-rise.

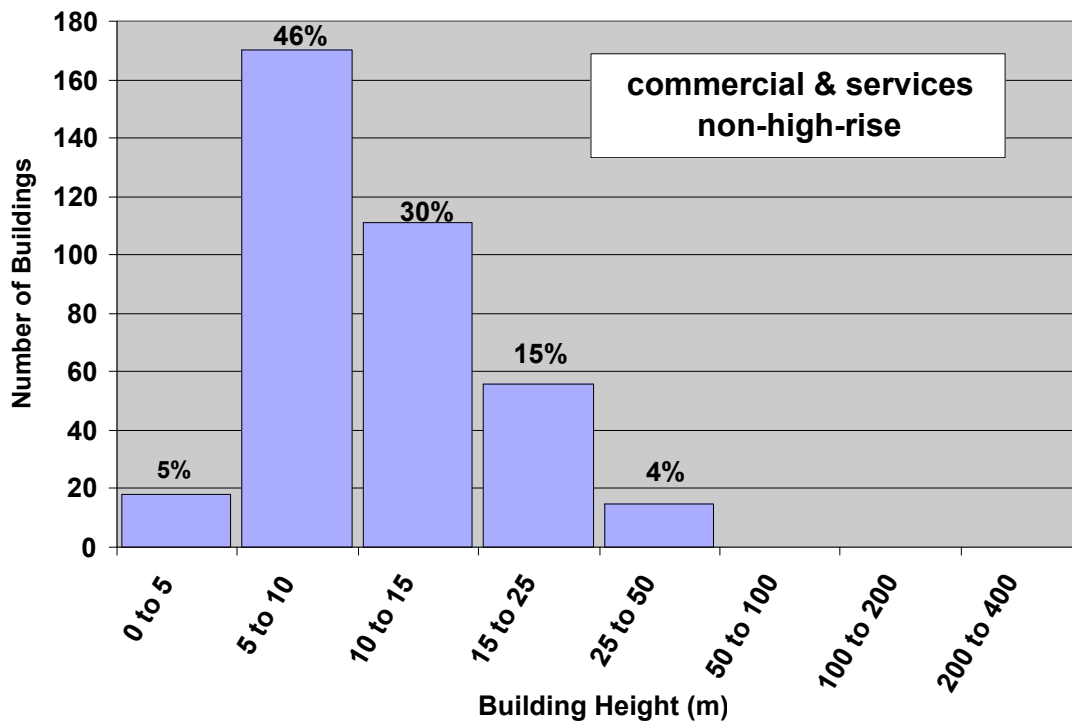


Figure 14. Distribution of building heights in the Commercial & Services Non-high-rise land use category.

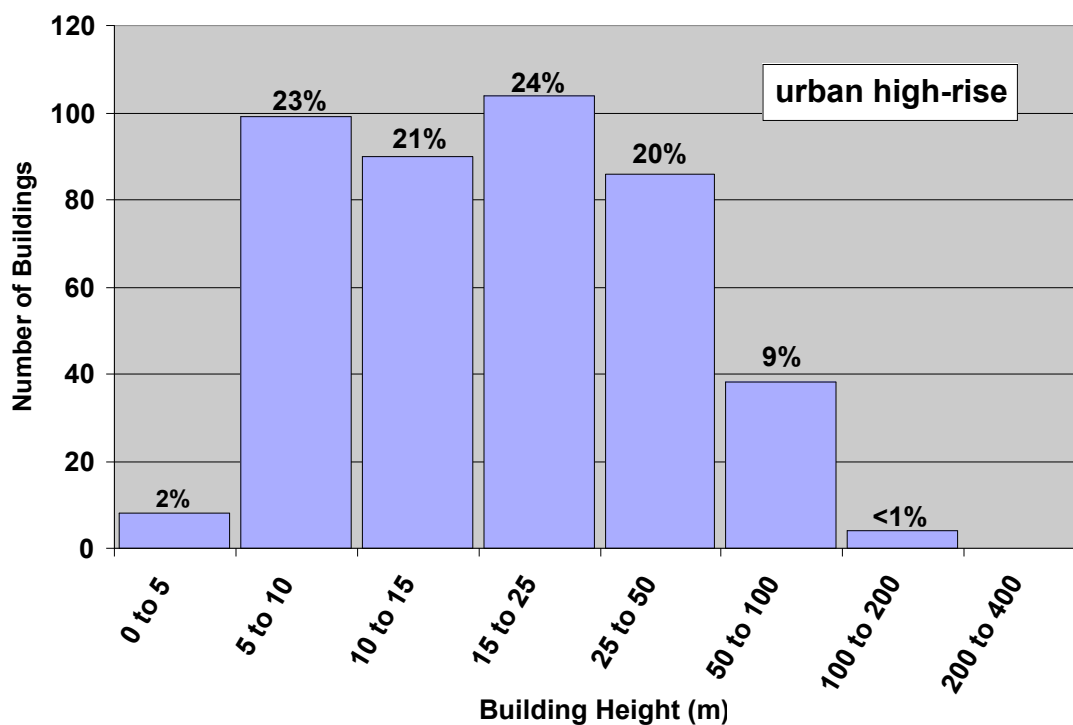


Figure 15. Distribution of building heights in the Urban High-rise land use category.

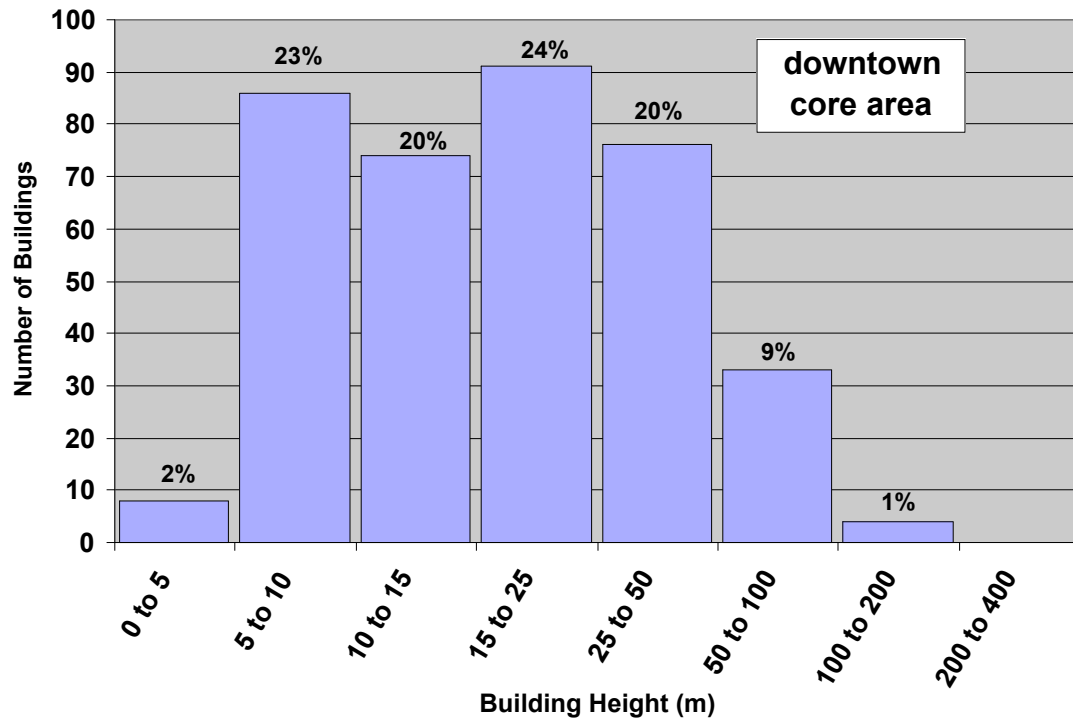


Figure 16. Distribution of building heights in the Downtown Core Area land use category.

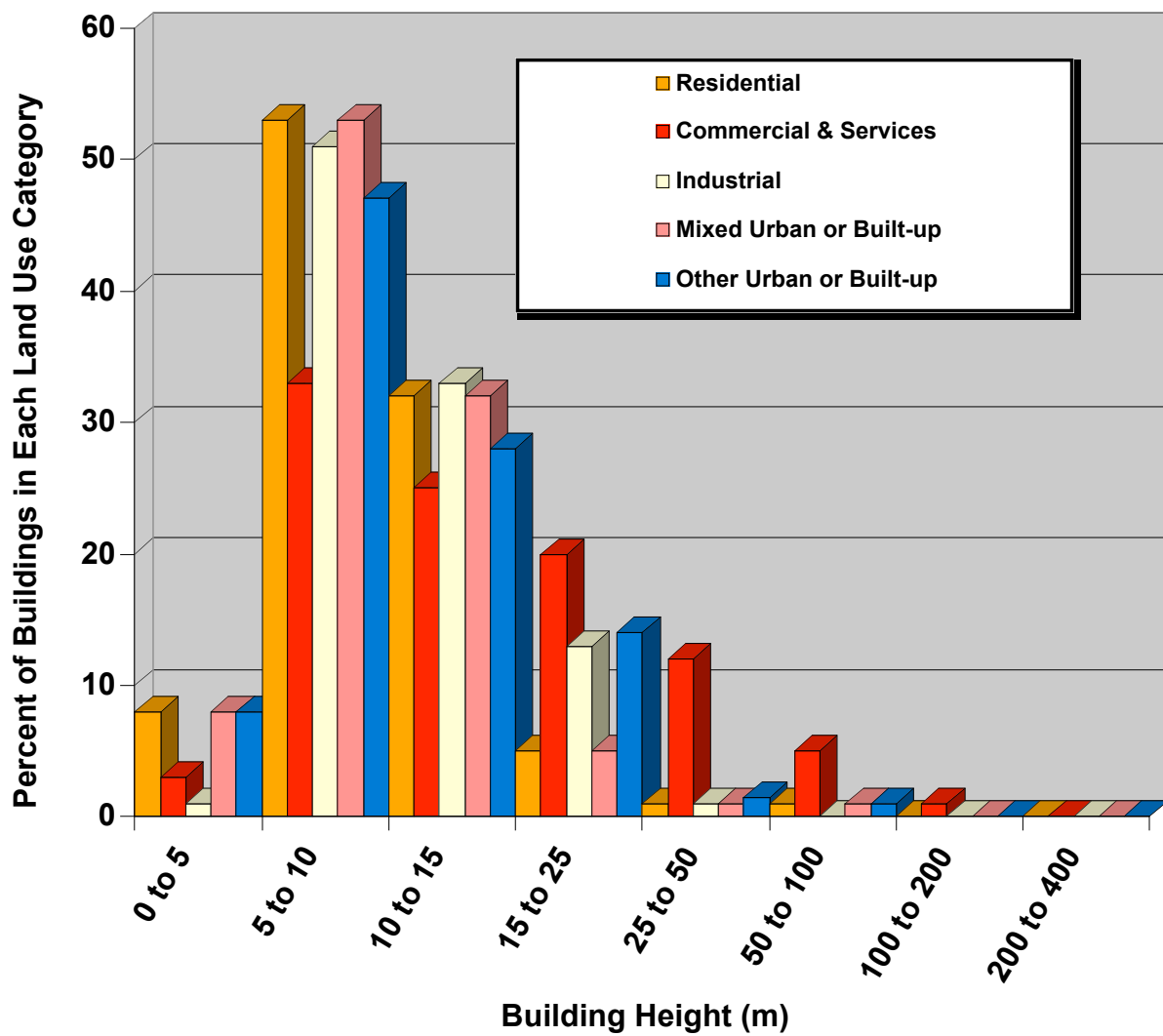


Figure 17. Comparison of the percent of buildings in each height increment for each 7-category land use type.

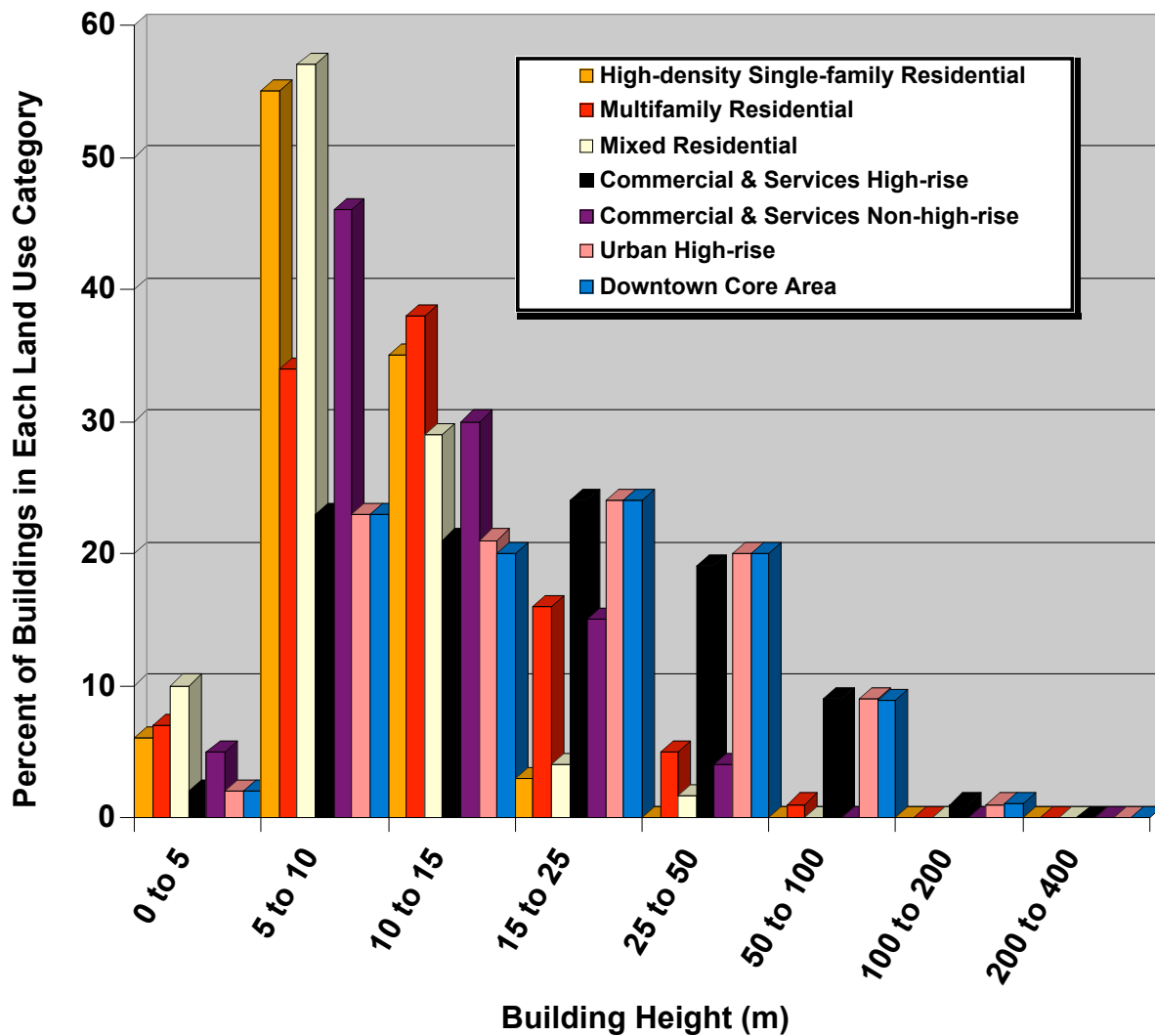


Figure 18. Comparison of the percent of buildings in each height increment for Residential and Commercial & Services subcategories and the special High-rise land use types.

Table 3 summarizes the building height characteristics as a function of land use. Several interesting features stand out. The buildings in the Residential land use average between 1 to 2 stories in height, but when plan area-weighted the average building height is closer to 3 stories. This observation possibly indicates that multi-story apartment buildings with large footprints are significant in this land use category, which is further supported by the number of buildings contained in the Multifamily and Mixed Residential land use categories. Table 3 also shows that the Industrial land use type is predominantly made up of shorter buildings (note the mean height of 10.8 m and the small standard deviation of 5.1 m), while Commercial & Services land use contains the taller buildings (mean height of 17.9 m and standard deviation of 16.5 m). The breakdown of Commercial & Services into High-rise and Non-high-rise categories shows that the average height of the Commercial & Services Non-high-rise is about 3-4 stories. The buildings in the Urban High-rise area of Salt Lake City have an average height of 23.5 m, and a

standard deviation of 20.3 m. Similarly, the buildings in the Downtown Core Area have an average height of 23.6 m, and a standard deviation of 20.3 m. The high-rise sections of Salt Lake City have relatively short buildings for a major U.S. city. For comparison, the average building height in the Downtown Core Area of Los Angeles is 45.0 m.

Table 3. Summary of building characteristics for the downtown Salt Lake City study area as a function of land use type.

Land Use Class	Number of Buildings	Average Height (m)	Standard Deviation	Plan Area-weighted Average Height (m)
Residential	1736	9.6	4.2	13.3
Low-density Single-family (< 8 units/hectare)	0	0	0	0
High-density Single-family (\geq 8 units/hectare)	639	9.3	2.9	9.9
Multifamily	249	11.0	11.6	16.6
Mixed	848	9.1	3.6	11.2
Commercial & Services	794	17.9	16.5	28.9
Non-high-rise	370	11.5	5.9	15.3
High-rise	424	23.4	20.3	40.4
Industrial	162	10.8	5.1	12.8
Transportation/Communications/Utilities	0	0	0	0
Mixed Industrial & Commercial	0	0	0	0
Mixed Urban or Built-up	191	11.2	7.1	15.4
Other Urban or Built-up	8	13.8	2.6	15.0
Predominantly Vegetated	3	11.4	1.6	12.4
Predominantly Built-up	5	15.8	1.9	15.7
Urban High-rise	429	23.5	20.3	40.5
Downtown Core Area	372	23.6	20.5	41.5

4.2 Building Plan Area Fraction (\square_p)

Background. Building plan area fraction has been shown to be related to the surface roughness z_0 (see Section 4.10). Surface roughness is used in air quality and meteorological models to account for enhanced mixing and drag effects of the rough surface. In the urban context, as the density of buildings (plan area fraction) increases so does the roughness of the system, but a threshold is eventually reached where adding new elements effectively reduces the drag of the elements present (Grimmond and Oke 1999). The density of buildings also indicates the potential flow regime. Hussain and Lee (1980) performed wind-tunnel experiments and found that three flow regimes develop in idealized urban street canyons: (1) isolated flow, (2) wake interference flow, and (3) skimming flow. The isolated flow regime occurs when elements are spaced relatively far apart ($0 < \square_p < 0.1$), the wake interference flow occurs when elements are spaced at a medium density level ($0.1 < \square_p < 0.6$), and the skimming flow regime occurs for high-density building arrangements ($\square_p > 0.6$) (Oke 1988).

Calculation Methods. The building plan area fraction (\square_p) is defined as the ratio of the plan area of buildings to the total surface area of the study region:

$$\square_p = \frac{A_p}{A_T} \quad (4)$$

where A_p is the plan area of buildings at ground level, i.e., the footprint area, and A_T is the total plan area of the region of interest, i.e., an arbitrary area that encompasses the buildings (see Figure 19). The computed value of the plan area fraction is dependent on the size of the area or the specific area in a city selected for the calculation. In most cases the plan area fraction will vary significantly from one city block to the next because of the heterogeneous nature of the urban landscape. The appropriate size of the calculation element should be chosen such that the characteristics of interest in the urban area are discernible.

Results. For the 6.1-km² study area the plan area fraction at ground level was calculated to be 0.23. This value is significantly lower than the plan area fraction of 0.47 found for Mexico City, Mexico (Grimmond and Oke 1999) and the 0.37 found for Vancouver, British Columbia, Canada (Voogt and Oke 1997), but more consistent with 0.30 found for Los Angeles (Burian et al. 2002b). This difference is partially due to the relatively wide streets and greater amounts of open space and parking lots around the buildings in downtown Salt Lake City compared to the downtown areas of the other major cities mentioned. Another reason might be the definition of the study area, which is defined for each city based on including the city center and a mixture of urban land use types (commercial, industrial, and residential), but is also constrained by cost of data purchases and time for data collection and analysis. The study area in Salt Lake City is larger than Mexico City and Vancouver and includes more residential areas.

We have calculated the plan area fraction on two meshes overlaid onto the study area in order to view the spatial heterogeneity. Figure 20 shows the two meshes overlaid onto land use: in the first case, a uniform 100-m X 100-m rectilinear grid cell mesh covering the entire 6.1-km² study area, and in the second case a non-uniform polygonal grid cell mesh based on the street network. As can be seen, the polygonal grids somewhat coincide with underlying land use type. Figure 21

shows the plan area fraction according to the two grid cell meshes. It is clear by comparison that there is significant variation within the polygonal meshes that follow the street network. The major highways running through the study area are clearly visible on the uniform mesh as open areas (low values of $\bar{\square}_p$). It is more difficult to see a one-to-one correlation with urban land use type, i.e., there appears to be significant variation in $\bar{\square}_p$ within an urban land use type. For example, in the industrial area in the southeast (gray region, Fig. 20), the plan area fraction ranges from high density to relatively open areas (Fig. 21).

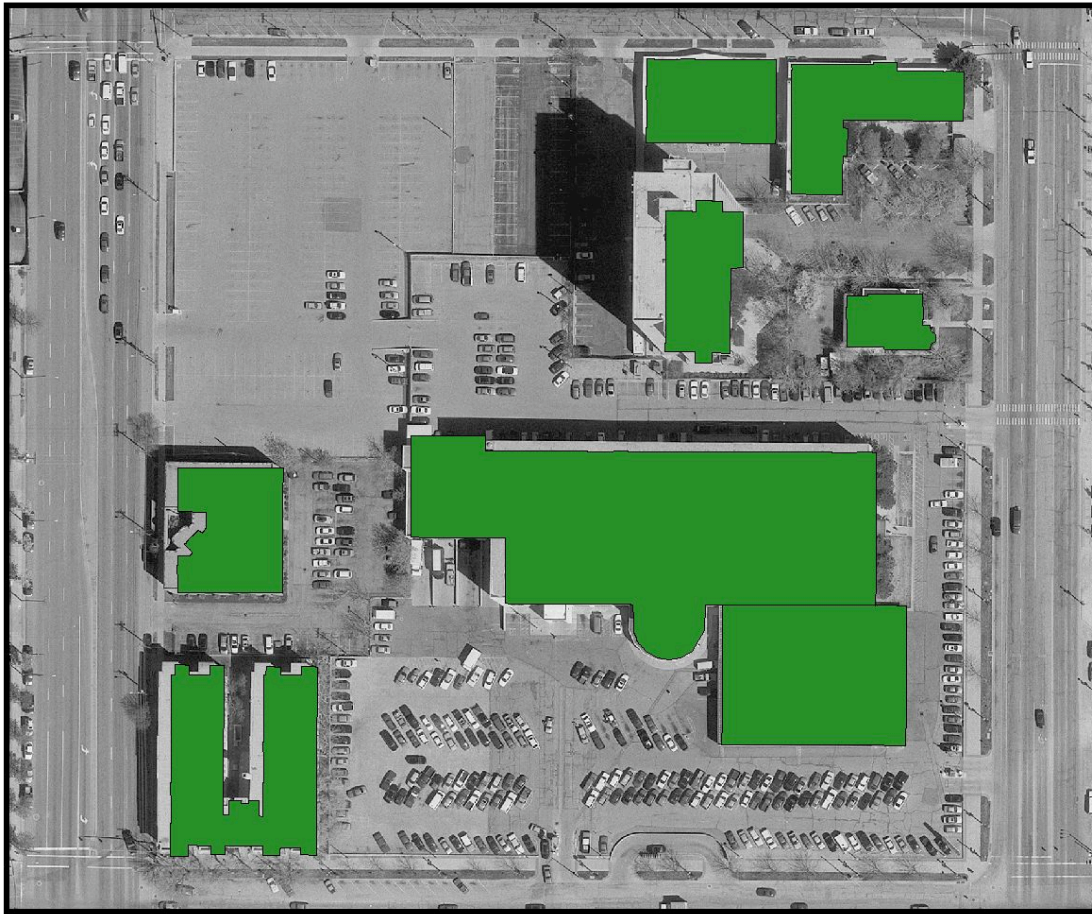


Figure 19. Illustration of building plan area fraction. The building plan area (A_p) in this scene is the sum of the areas of the building footprints shown in green. The total plan area (A_T) is the area enclosed by the outline of the figure. The building plan area fraction ($\bar{\square}_p$) is computed by dividing building plan area (A_p) by total plan area (A_T).



Figure 20. Grid cells used to display and analyze the spatial heterogeneity of the Salt Lake City building morphology for the 6.1-km² study area. Urban land use type overlaid with (a) the 100-m X 100-m uniform grid cell mesh, and (b) the non-uniform grid cells based on street network.

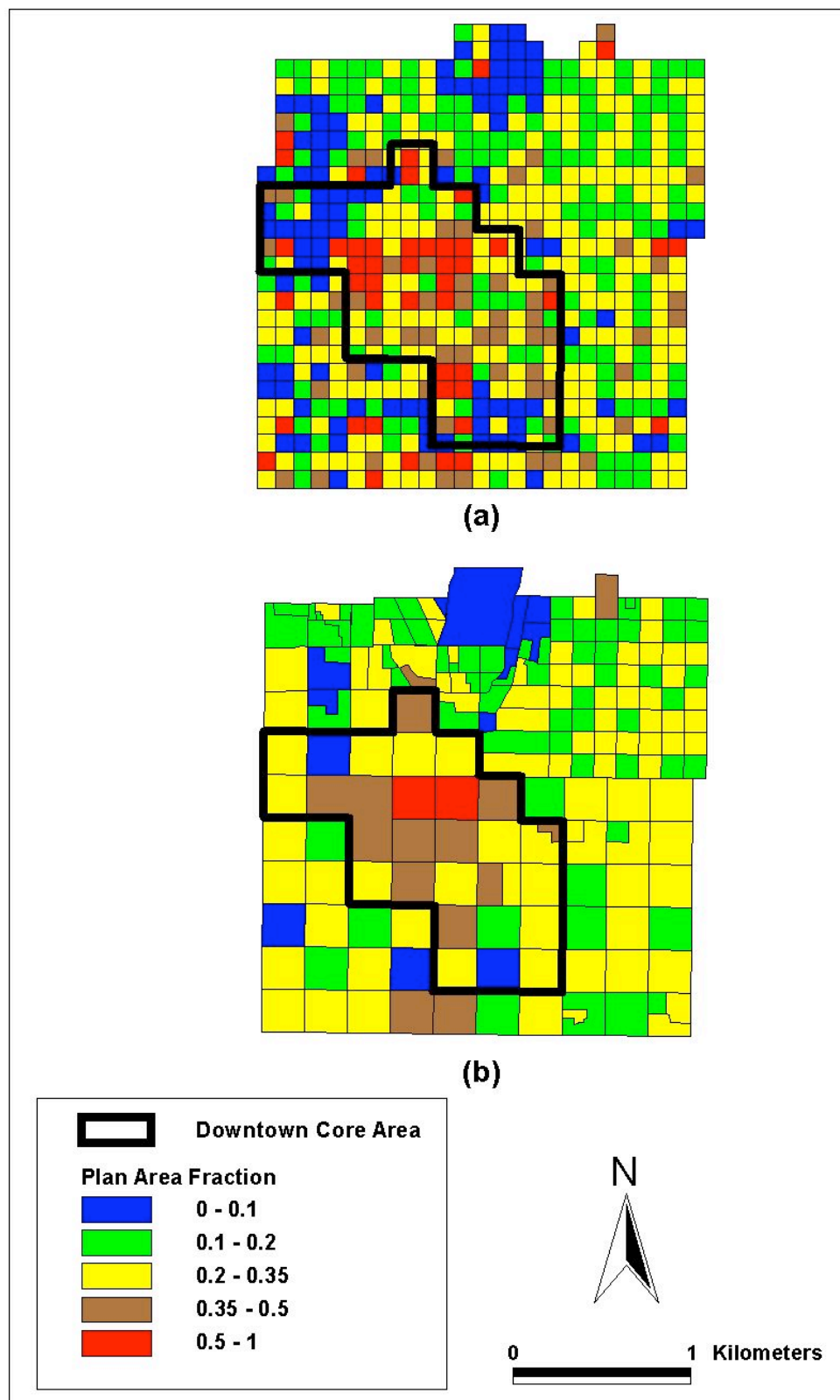


Figure 21. Spatial variability of building plan area fraction (\bar{p}_b) distributed according to a uniform 100-m X 100-m grid mesh and a non-uniform grid mesh based on the downtown road network.

Table 4 contains the computed $\bar{\lambda}_p$ for each land use type in the land use classification schemes described in Section 3.2. Table 4 indicates that the Industrial and the Commercial & Services land use categories have a significantly higher density than the other land use types. The Other Urban or Built-up land use contains only a few buildings and hence has a low plan area fraction. Surprisingly, the plan area fraction for the Residential areas is nearly the same as the Commercial & Services land use type, but one should recall that in our study area all Residential land use is high density. Most of the average values shown in Table 4 fall within the $\bar{\lambda}_p$ range for wake interference flow ($0.1 < \bar{\lambda}_p < 0.6$) (Hussain and Lee 1980).

Table 4. Plan area fraction as a function of land use type

Land Use Class	$\bar{\lambda}_p$
Residential	0.21
Low-density Single-family (< 8 units/hectare)	---
High-density Single-family (≥ 8 units/hectare)	0.19
Multifamily	0.25
Mixed	0.21
Commercial & Services	0.27
Non-high-rise	0.20
High-rise	0.32
Industrial	0.27
Transportation/Communications/Utilities	---
Mixed Industrial & Commercial	---
Mixed Urban or Built-up	0.19
Other Urban or Built-up	0.02
Predominantly Vegetated	0.00
Predominantly Built-up	0.09
Urban High-rise	0.23
Downtown Core Area	0.33

In Table 5, we compare the computed plan area fraction values for several land use types in Salt Lake City to those reported in other studies. Our computed values of $\bar{\lambda}_p$ for Residential and Industrial land use types are smaller than those of other cities. The plan area fraction values computed in these other studies have included the plan area of trees in residential areas, which can be a significant fraction of the plan area. Trees are not included in our calculations of $\bar{\lambda}_p$ and explain some of the differences. However, visual inspection of aerial photos suggests that there are relatively few trees and shrubs in the high-density residential areas in our study region. The relatively low values for the Salt Lake City downtown area can be attributed to the small footprint of the downtown core area high rises and the large amount of car habitat (e.g., wide roadways, parking lots, driveways) present in the downtown Salt Lake City area, which effectively limits the amount of buildings and minimizes the open space available for trees and shrubs.

Table 5. Comparison of plan area fraction (\bar{f}_p) for downtown Salt Lake City to other cities. Locations grouped by land use type and then listed in order of decreasing \bar{f}_p .

Location	Land Use Class	\bar{f}_p	Source
Vancouver, BC, Canada	Suburban Residential	0.62	Voogt and Oke (1997)
Sacramento, CA	Suburban Residential	0.58	Grimmond and Oke (1999)
Arcadia, CA	Suburban Residential	0.53	Grimmond and Oke (1999)
Chicago, IL	Suburban Residential #1	0.47	Grimmond and Oke (1999)
Chicago, IL	Suburban Residential #2	0.38	Grimmond and Oke (1999)
San Gabriel, CA	Suburban Residential	0.36	Grimmond and Oke (1999)
Miami, FL	Suburban Residential	0.35	Grimmond and Oke (1999)
Tucson, AZ	Suburban Residential	0.33	Grimmond and Oke (1999)
Los Angeles, CA	Mixed Residential	0.29	Burian et al. (2002b)
Los Angeles, CA	High-density Single-family Residential	0.27	Burian et al. (2002b)
Salt Lake City, UT	High-density Single-family Residential	0.19	This report
Los Angeles, CA	Industrial	0.38	Burian et al. (2002b)
Vancouver, BC, Canada	Light Industrial	0.38	Voogt and Oke (1997)
Salt Lake City, UT	Industrial	0.27	This report
Mexico City, Mexico	Downtown	0.47	Grimmond and Oke (1999)
Vancouver, BC, Canada	Downtown	0.37	Voogt and Oke (1997)
Salt Lake City, UT	Downtown Core Area	0.33	This report
Los Angeles, CA	Urban High-rise	0.32	Burian et al. (2002b)
Los Angeles, CA	Downtown Core Area	0.29	Burian et al. (2002b)

4.3 Building Plan Area Density ($a_p(z)$)

Background. The building plan area density gives information on how much of the air volume is occupied by buildings (when multiplied by the height increment of the volume of interest). The change in building plan area density with height yields the roof fraction (see Section 4.4). The roof fraction is important from a thermodynamic perspective because of the significant solar gain and heat loss there. The building plan area density can be used to derive the roof area density, which is analogous to the leaf area density. The leaf area density gives information on how much long- and short-wave radiation travels through the canopy and how much is intercepted. Something similar might be done for urban areas with buildings using the building plan area density. Building plan area density can also be used as a surrogate for frontal area density (see Section 4.5) in evaluating the drag force as a function of height due to buildings in urban areas.

Calculation Methods. The building plan area density ($a_p(z)$) is defined as the average building plan area within a height increment divided by the volume of the height increment:

$$a_p(z) = \frac{\frac{1}{\Delta z} \int_{z-\frac{1}{2}\Delta z}^{z+\frac{1}{2}\Delta z} A_p(z') dz'}{A_T \Delta z} \quad (5)$$

where, $A_p(z')$ is the plan area of buildings at height z' , A_T is the plan area of the site, and Δz is the height increment for the calculation. Since A_T is not a function of height we can bring it into the integral in the numerator and obtain:

$$a_p(z) = \frac{\frac{1}{\Delta z} \int_{z-\frac{1}{2}\Delta z}^{z+\frac{1}{2}\Delta z} \frac{A_p(z')}{A_T} dz'}{\Delta z} \quad (6)$$

Knowing $\overline{A_p(z')} = A_p(z')/A_T$ and assuming that the building plan area does not change appreciably within a height increment Δz , eq. (6) can be approximated by:

$$a_p(z) \approx \frac{\overline{A_p(z)}}{\Delta z} \quad (7)$$

Results. Figure 22 illustrates the building plan area density function ($a_p(z)$) for the Salt Lake City study area using a 1-m height increment. As expected, $a_p(z)$ is constant for the first few meters above ground elevation until the rooftop height of the shortest buildings are reached (approximately four meters). Building plan area density then rapidly declines with height and

asymptotically approaches $\bar{\rho}_p = 0$. Only the first 100 m above ground elevation are shown because $a_p(z)$ is nearly zero above this height.

Figure 23 shows $a_p(z)$ for the 7-category land use scheme. The plot does not contain the building plan area density for the Other Urban or Built-up land use because this land use does not contain enough buildings to produce meaningful results. The building plan area density of the Industrial and Residential land uses decreases relatively rapidly with height above four meters, indicating that these land use categories contain mostly two and three story buildings. The $a_p(z)$ for the Commercial & Services land use is the largest near the ground, indicating that the buildings in this land use type have a large footprint and are densely packed. Figure 24 shows $a_p(z)$ for several land use types in the 12-category scheme, as well as the Urban High-rise and Downtown Core Area land uses. The plot shows that the $a_p(z)$ associated with Commercial & Services Non-high-rise decreases much more rapidly with height than the Commercial & Services High-rise land use type and is very similar in nature to the Multifamily Residential. It is clear that the Commercial & Services land use type (found in the USGS LULC database) is composed of two distinct classes of buildings.

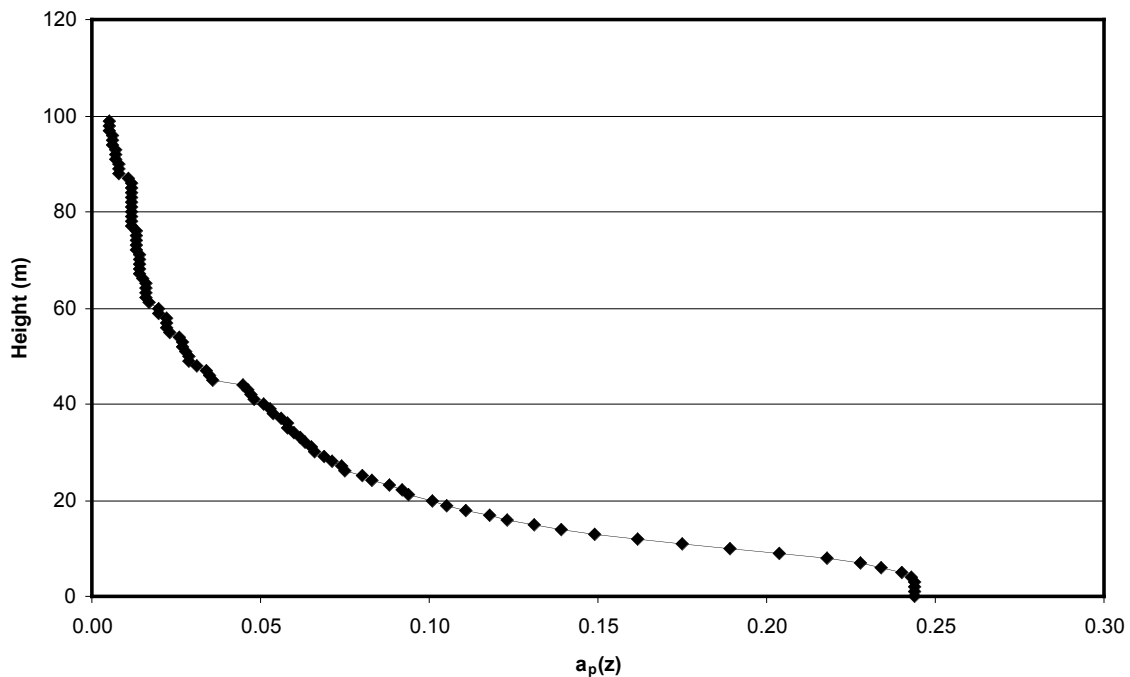


Figure 22. Building plan area density function ($a_p(z)$) for the entire 6.1-km² downtown Salt Lake City area.

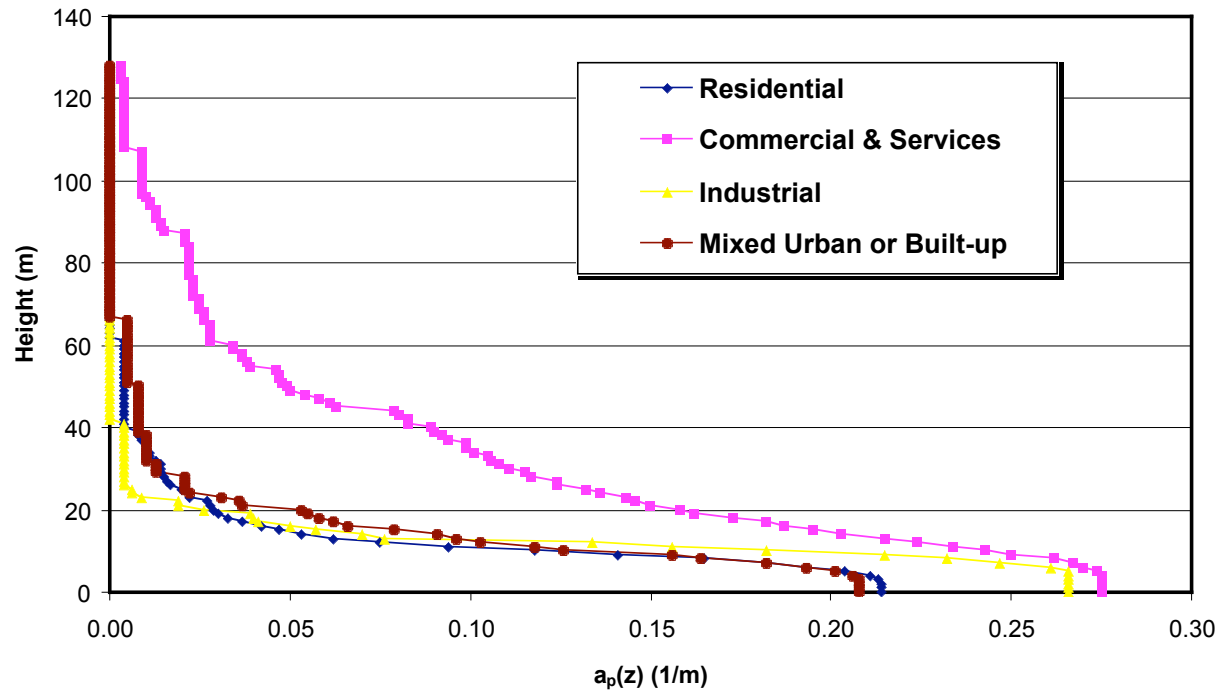


Figure 23. Building plan area density function ($a_P(z)$) for four of the land use classes in the 7-category classification scheme.

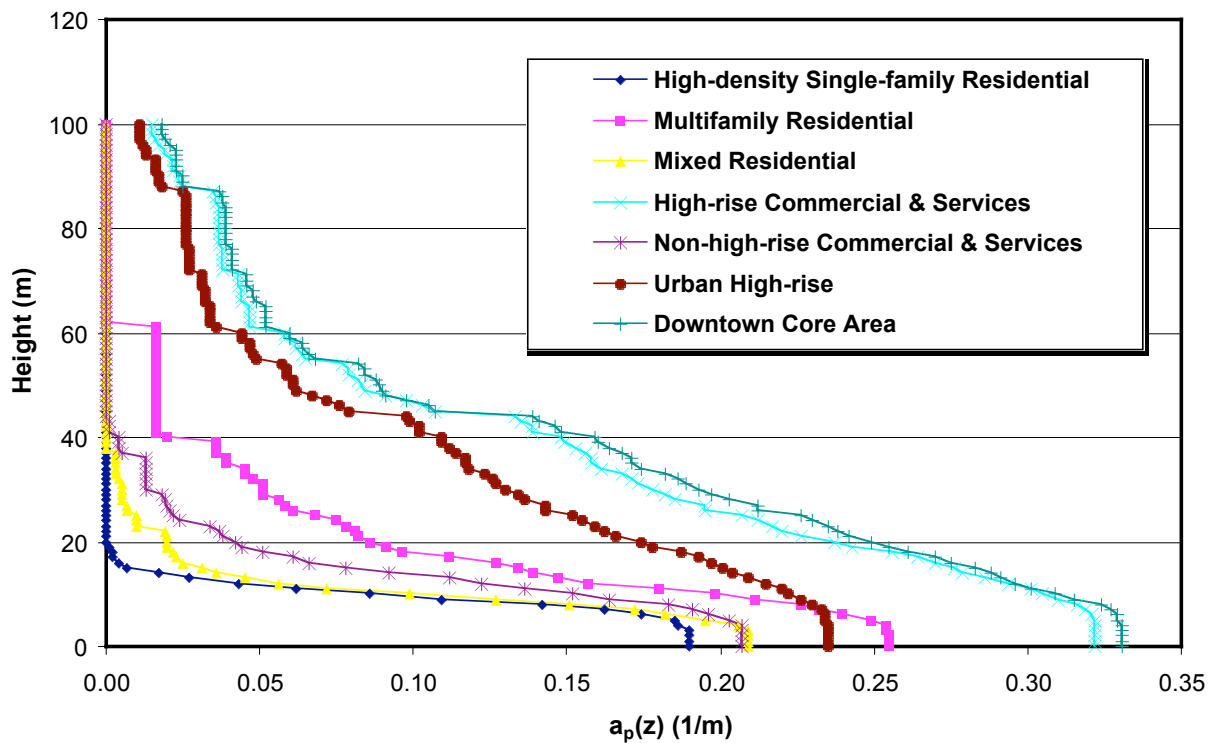


Figure 24. Building plan area density function ($a_P(z)$) for several land use types in the 12-category scheme and the Urban High-rise and Downtown Core Area land uses.

4.4 Roof Area Density ($a_r(z)$)

Background. The rooftop area as a function of a height is important in describing the thermodynamics of the urban canopy. Roofs are interceptors and reflectors of solar radiation, and give off or absorb long-wave radiation. Knowledge of the roof area, therefore, is important in determining the energy balance within the urban canopy. The roof area density is a quantity that can be used to compute roof area as a function of height. The roof area density is analogous to the leaf area density. The leaf area density can be integrated from the top of the vegetative canopy to the ground to yield a leaf area index. The leaf area index gives information on how much long- and short-wave radiation travels through the canopy and how much is intercepted. Roof area density might be used in a similar fashion to help estimate energy fluxes through the urban canopy.

Calculation Methods. The rooftop area within a height increment Δz can be approximated by the difference between the building plan areas at two heights:

$$A_r(z) = A_p\left(\frac{z}{2}\right) - \frac{\Delta z}{2} \frac{dA_p}{dz} + \frac{\Delta z}{2} \frac{dA_p}{dz} \quad (8)$$

where $A_p(z)$ is the plan area of buildings at the specified height and a flat-roofed assumption has been made. The roof area density ($a_r(z)$) can then be defined as the rooftop plan area per height increment Δz divided by the volume of the height increment:

$$a_r(z) = \frac{A_r(z)}{A_T \cdot \Delta z} = \frac{A_p\left(\frac{z}{2}\right) - \frac{\Delta z}{2} \frac{dA_p}{dz} + \frac{\Delta z}{2} \frac{dA_p}{dz}}{A_T \cdot \Delta z} \quad (9)$$

where A_T is the total area within which buildings are contained. Analogous to the leaf area index used in the plant canopy community, the integration of $a_r(z)$ from a specified elevation above ground (z) to the height of the canopy (h_c) is equal to the building area index ($L(z)$):

$$L(z) = \int_z^{h_c} a_r(z) dz \quad (10)$$

The integration of $a_r(z)$ from ground elevation to the canopy height (h_c) is equal to L_p :

$$L(0) = L_p = \int_0^{h_c} a_r(z) dz \quad (11)$$

Results. The roof area density function $a_r(z)$ is shown in Figure 25 for the Salt Lake City study area. A significant fraction of the rooftop area is located within the first 10 meters of height above ground. The value of $a_r(z)$ is zero below 3 m because no buildings are defined to be below 3 meters (approximately one story) in height. Figures 26 and 27 show $a_r(z)$ for the 7-category land use scheme and for the 12-category scheme along with the Urban High-rise and Downtown Core Area land use types, respectively. Figure 26 is limited to the first 60 meters and Figure 27

is limited to the first 100 meters of height to make them more readable because for most of the land use types the first 60-100 meters of height contains all the rooftop area. The Residential and Industrial land uses consistently have the largest rooftop density fraction within 5-10 meters of the ground, whereas the Commercial & Services Non-high-rise land use and the Urban High-rise generally have a more consistent distribution of roof area density at low heights continuing to 50 to 60 meters.

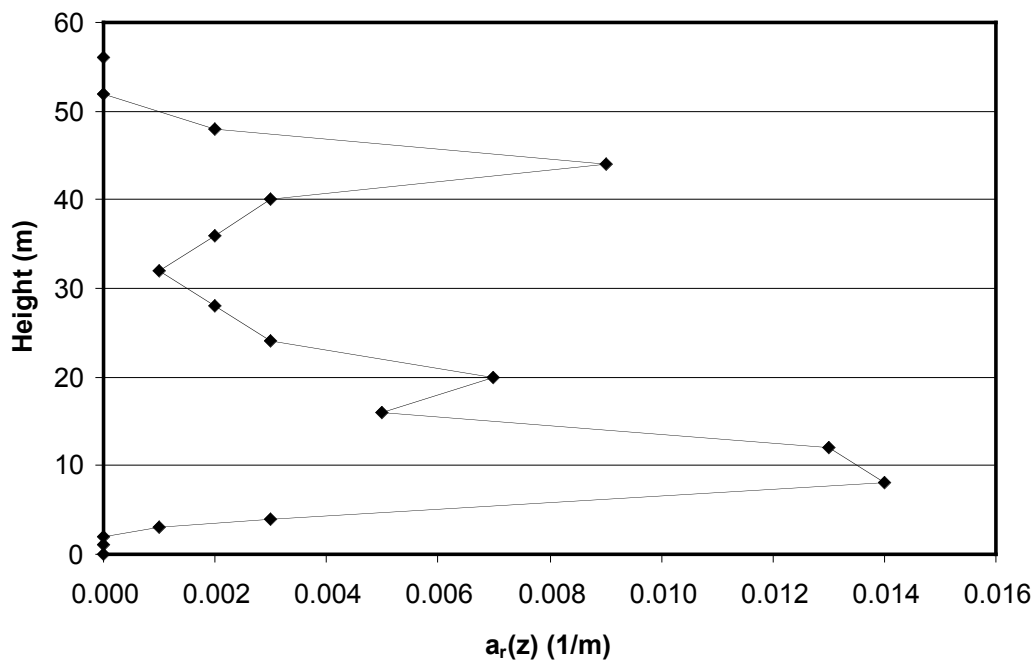


Figure 25. Roof area density function ($a_r(z)$) for the Salt Lake City study area. Data are plotted for 1-m height increments up to 4 m and then by 4-m increments (approximately one story) up to 60 m.

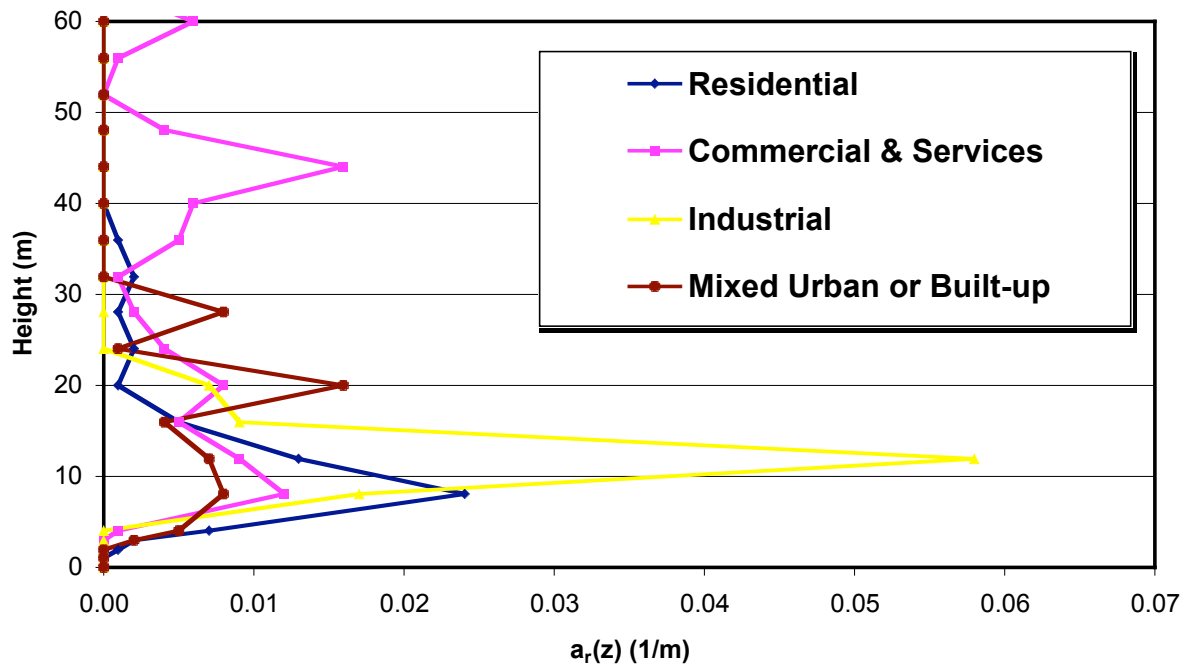


Figure 26. Roof area density function ($a_r(z)$) for the 7-category land use scheme. Data are plotted for 1-m height increments up to 4 m and then by 4-m increments (approximately one story) up to 60 m.

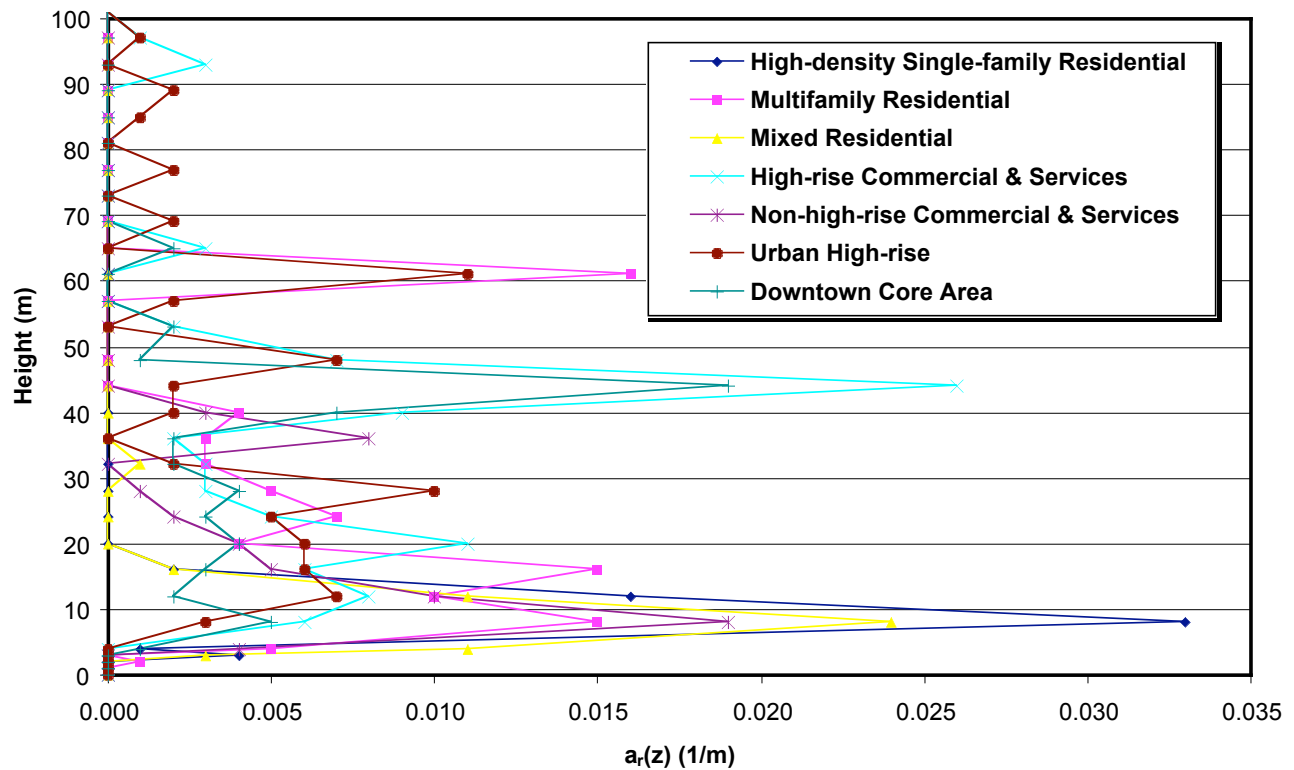


Figure 27. Roof area density function ($a_r(z)$) for the level 2 land use types and Urban High-rise and Downtown Core Area. Data are plotted for 1-m height increments up to 4 m and then by 4-m increments (approximately one story) up to 100 m.

4.5 Building Frontal Area Index (\bar{F}_f)

Background. Building walls facing into the wind impart drag on the air flow. The frontal area index, a measure of the frontal area per unit horizontal area, has been shown to be related to the surface roughness z_0 (see Section 4.10). Surface roughness is used in air quality and meteorological models to account for enhanced mixing and the drag effects of the rough surface. The flow regime within urban street canyons is also thought to be a function of the frontal area index and plan area fraction (see Section 4.2).

Calculation Methods. The frontal area index (\bar{F}_f) is defined as the total area of buildings projected into the plane normal to the approaching wind direction (A_{proj}) divided by the plan area of the study site (A_T):

$$\bar{F}_f(\theta) = \frac{A_{proj}}{A_T} \quad (12)$$

where θ is the wind direction. Figure 28 illustrates frontal area. An Avenue script was written for use in the ArcView GIS to automatically determine the total area of building surfaces in the projected plane normal to a specified wind direction (A_{proj}) and calculate \bar{F}_f using Eqn. (12).

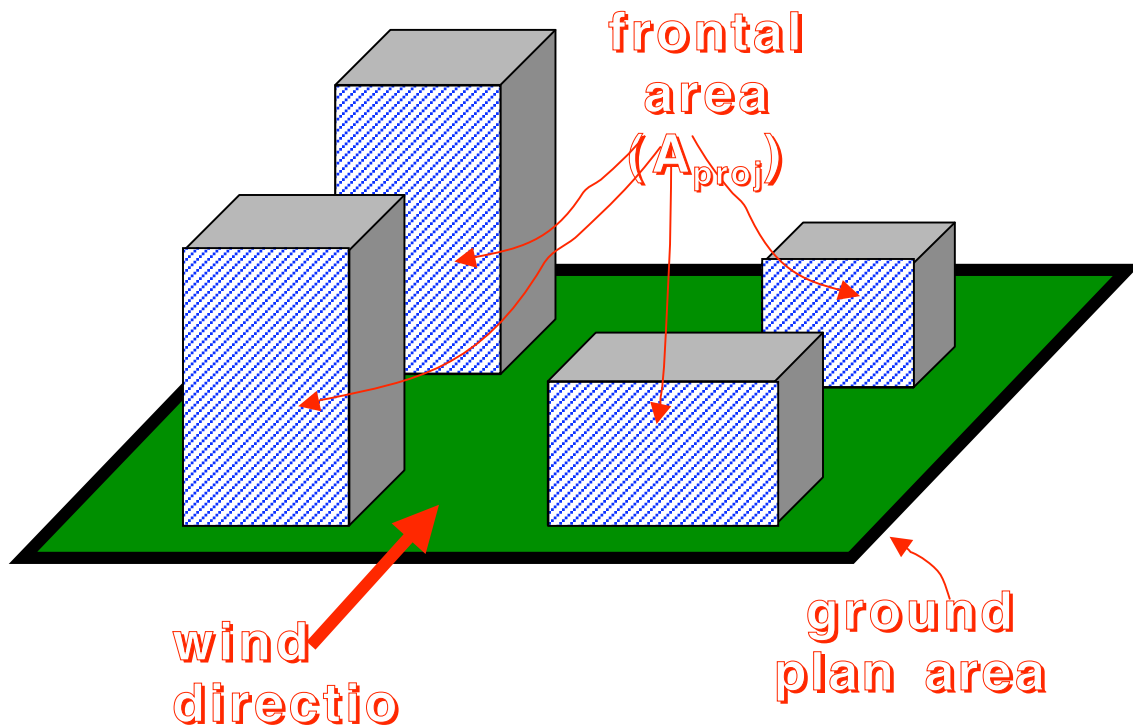


Figure 28. Illustration of projected frontal area. In the schematic of the four buildings shown above, the frontal area (A_{proj}) is the total area of the faces exposed to the oncoming wind.

The frontal area index (\square_f) can be approximated from the product of mean height, breadth, and density of roughness elements (Grimmond and Oke 1999):

$$\square_f = \overline{L_y} \overline{H} \square_d \quad (13)$$

where $\overline{L_y}$ is the mean breadth of the roughness elements perpendicular to the wind direction, \overline{H} is the mean roughness element height, and \square_d is the density (number) of roughness elements per unit area ($\square_d = n/A_T$).

Similar to the plan area fraction \square_p , the value of \square_f will be dependent on the location and the size of the area selected for analysis. Therefore, we have calculated \square_f for several different sized areas and as a function of land use. In addition, there is some ambiguity regarding the minimum distance between two adjacent buildings that should be used to distinguish the buildings as two separate buildings. The issue is that as two buildings are placed closer together the upstream building may start to mask the frontal face of the downstream building. For some applications, knowing the exposed frontal area may be more important than knowing the total frontal area. For example, for a cluster of buildings the drag may be better correlated to exposed frontal area as compared to total frontal area. For this study, we consider two separate buildings to be a single building only if the adjacent faces are touching. Using this rule we calculated the \square_f using the Avenue scripts for the entire 6.1-km² study area assuming the wind was approaching the city from the north, northeast, east, southeast, south, southwest, west, and northwest.

Results. Table 6 lists the computed \square_f values for the 6.1-km² study area for eight approach wind directions. For this large study area (i.e., an area with many buildings) \square_f is only slightly sensitive to approach flow wind direction. Because of the symmetrical characteristics of buildings it is expected that opposite wind directions (e.g., North and South) will have nearly identical frontal area indices. For our study area, the majority of streets run in the N-S and E-W directions. Hence, the along street directions are north, east, south, and west directions and have slightly smaller values.

Table 6. Summary of frontal area index (\square_f) for downtown Salt Lake City for several wind approach directions.

	North	Northeast	East	Southeast	South	Southwest	West	Northwest
\square_f	0.178	0.240	0.170	0.239	0.178	0.240	0.170	0.239

The value of \square_f is expected to be a function of land use because of the differences in building characteristics between different land uses. The relationship is also expected to be variable for samples of the same type of land use where building characteristics are highly variable, e.g., Urban High-rise, but not so variable for fairly homogeneous and consistent land uses, e.g.,

Single-family High-density Residential. Table 7 shows the \overline{F}_f values calculated for each land use type. Table 8 compares the computed \overline{F}_f for several land uses in Salt Lake City to the computed \overline{F}_f for other cities and land uses. Note that we have not included trees in our calculation of the frontal area index, but several of the other studies cited in Table 8 have included trees.

Figure 29 shows the frontal area index for a north wind azimuth spatially distributed according to the non-uniform grid cell mesh. Calculations were not possible for the uniform 100-m X 100-m mesh because the grid cells are smaller than several buildings and buildings cross grid cell boundaries. This causes problems when trying to calculate the projected wall area in the grid cell. Some cells do not contain any walls because they are completely within the building. Rather than trying to develop a method to calculate \overline{F}_f for these instances we decided to forego the calculation of \overline{F}_f for the uniform grid cell mesh. Similar to the plan area fraction, we see smaller frontal area index values computed for areas including highway. Different from the plan area fraction distribution, we see the highest computed frontal area index values in the high-rise city center area, and lower values in the industrial regions. In general, the study area has a significant variation in computed frontal area index values. Several grid cells have computed values near zero, while several have computed values greater than 0.5. A direct relationship between land use and frontal area index is not demonstrated in this study area. Although we note the general trend of higher than average frontal area index values in the high-rise areas, this is not universal. For example, several grid cells contain tall buildings with small plan area fractions compared to the grid cell plan area, which results in a smaller than average frontal area index.

Table 7. Frontal area index (\overline{F}_f) as a function of land use type.
Four approach wind directions are included in the table.

Land Use Class	North	Northeast	East	Southeast
Residential	0.175	0.240	0.173	0.238
Low-density Single-family (< 8 units/hectare)	---	---	---	---
High-density Single-family (\geq 8 units/hectare)	0.168	0.230	0.164	0.229
Multifamily	0.204	0.289	0.222	0.282
Mixed	0.165	0.222	0.156	0.222
Commercial & Services	0.204	0.272	0.190	0.271
Non-high-rise	0.102	0.140	0.099	0.140
High-rise	0.281	0.370	0.258	0.367
Industrial	0.117	0.167	0.127	0.167
Transportation/Communications/Utilities	---	---	---	---
Mixed Industrial & Commercial	---	---	---	---
Mixed Urban or Built-up	0.135	0.184	0.132	0.184
Other Urban or Built-up	0.012	0.017	0.012	0.017
Predominantly Vegetated	0.003	0.005	0.003	0.005
Predominantly Built-up	0.061	0.085	0.061	0.085
Urban High-rise	0.278	0.366	0.256	0.363
Downtown Core Area	0.170	0.223	0.155	0.222

Table 8. Comparison of frontal area index (\bar{F}_f) for several cities and land uses

Location	Land Use Class	\bar{F}_f	Source
Arcadia, CA	Suburban residential	0.33	Grimmond and Oke (1999)
Chicago, IL	Suburban residential	0.28	Grimmond and Oke (1999)
Los Angeles, CA	Multifamily residential	0.25	Burian et al. (2002b)*
Salt Lake City, UT	Multifamily residential	0.25	This report*
Sacramento, CA	Suburban residential	0.23	Grimmond and Oke (1999)
Chicago, IL	Suburban residential	0.21	Grimmond and Oke (1999)
Tucson, AZ	Suburban residential	0.19	Grimmond and Oke (1999)
Vancouver, BC, Canada	Suburban residential	0.19	Grimmond and Oke (1999)
Miami, FL	Suburban residential	0.16	Grimmond and Oke (1999)
San Gabriel, CA	Suburban residential	0.14	Grimmond and Oke (1999)
Los Angeles, CA	High-density single-family residential	0.12	Burian et al. (2002b)*
Salt Lake City, UT	Industrial	0.15	This report*
Vancouver, BC, Canada	Light Industrial	0.13	Grimmond and Oke (1999)
Los Angeles, CA	Industrial	0.10	Burian et al. (2002b)*
Los Angeles, CA	Urban high-rise	0.45	Burian et al. (2002b)*
Los Angeles, CA	Downtown core area	0.38	Burian et al. (2002b)*
Salt Lake City, UT	Urban high-rise	0.32	This report*
Vancouver, BC, Canada	Central city	0.30	Grimmond and Oke (1999)
Mexico City, Mexico	Central city	0.19	Grimmond and Oke (1999)
Los Angeles, CA	Non-high-rise commercial & services	0.13	Burian et al. (2002b)*

*The values shown from this study are the average values for eight wind directions (north, northeast, east, southeast, south, southwest, west, northwest).

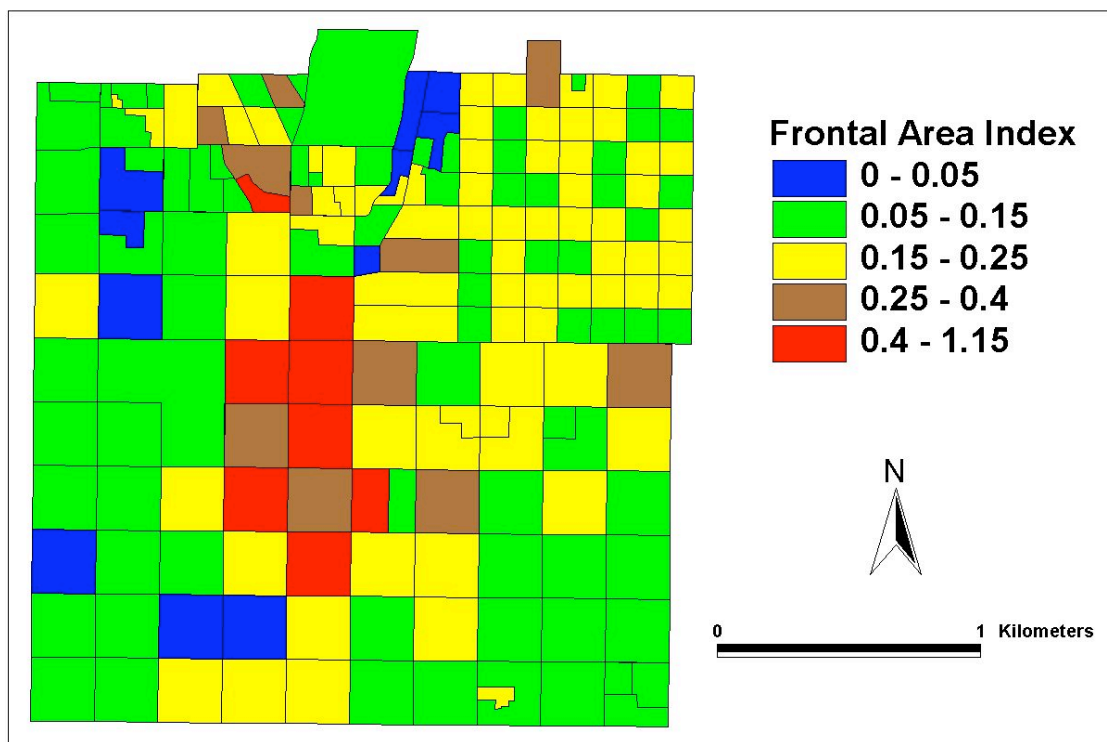


Figure 29. Spatial distribution of building frontal area index (\bar{a}_f) for a north wind azimuth.

4.6 Frontal Area Density ($a_f(z)$)

Background. The frontal area is often used in computing the drag force on solid objects immersed in fluids. The frontal area density, a measure of the frontal area per unit horizontal area per unit height increment, has been used by researchers in the plant canopy and urban canopy communities to help quantify the drag force as a function of height. The drag force approach allows one to compute the area-averaged wind profile within the canopy.

Calculation Methods. The frontal area density ($a_f(z)$) is defined as:

$$a_f(z, \varphi) = \frac{A(\varphi)_{proj(\varphi z)}}{A_T \Delta z} \quad (14)$$

where $A(\varphi)_{proj(\varphi z)}$ is the area of building surfaces projected into the plane normal to the approaching wind direction for a specified height increment (Δz), φ is the wind direction angle, and A_T is the total plan area of the study site. For a specified wind direction, the integral of $a_f(z)$ over the canopy height equates to \bar{a}_f .

Results. We performed the frontal area density calculations at one-meter increments. Figure 30 shows $a_f(z)$ for the Salt Lake City study area for a wind approaching from the north. Figure 31 shows the $a_f(z)$ functions for the land use types in the 7-category scheme that have a sufficient number of buildings and land area to produce meaningful results. Figure 32 shows the $a_f(z)$ functions for the 12-category land use scheme and the Urban High-rise and Downtown Core Area land uses.

Interestingly, the frontal area density near the ground is largest for Residential areas. This occurs due to the preponderance of shorter buildings in Residential areas (many short buildings occupying the same volume as a few taller buildings have more frontal area). Industrial land use has relatively high frontal area density near the ground as well, greater than Commercial & Services. Presumably Commercial & Services Non-high-rise has a relatively low frontal area density near the surface due to wide, squat buildings, like shopping centers and strip malls with large open parking lots. The frontal area density decays most rapidly with height for Residential and Industrial areas due to low building heights. The Urban High-rise land use decays most slowly with height due to the large number of tall buildings in this land use type.

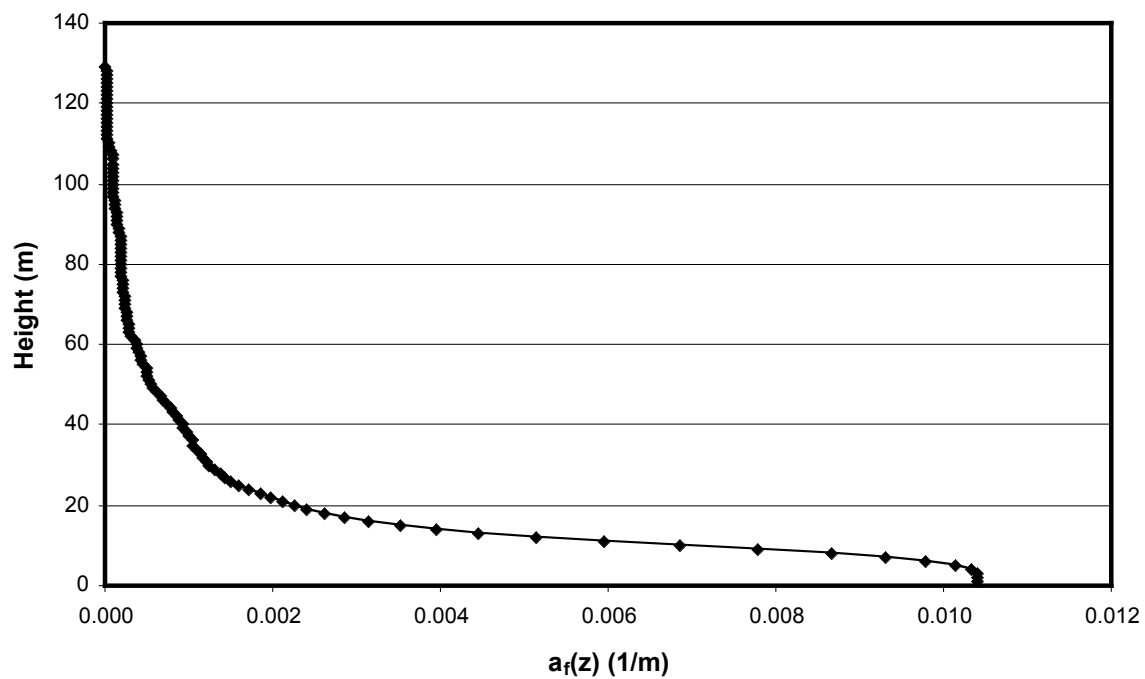


Figure 30. Frontal area density function ($a_f(z)$) for the Salt Lake City study area for a wind approaching from the north.

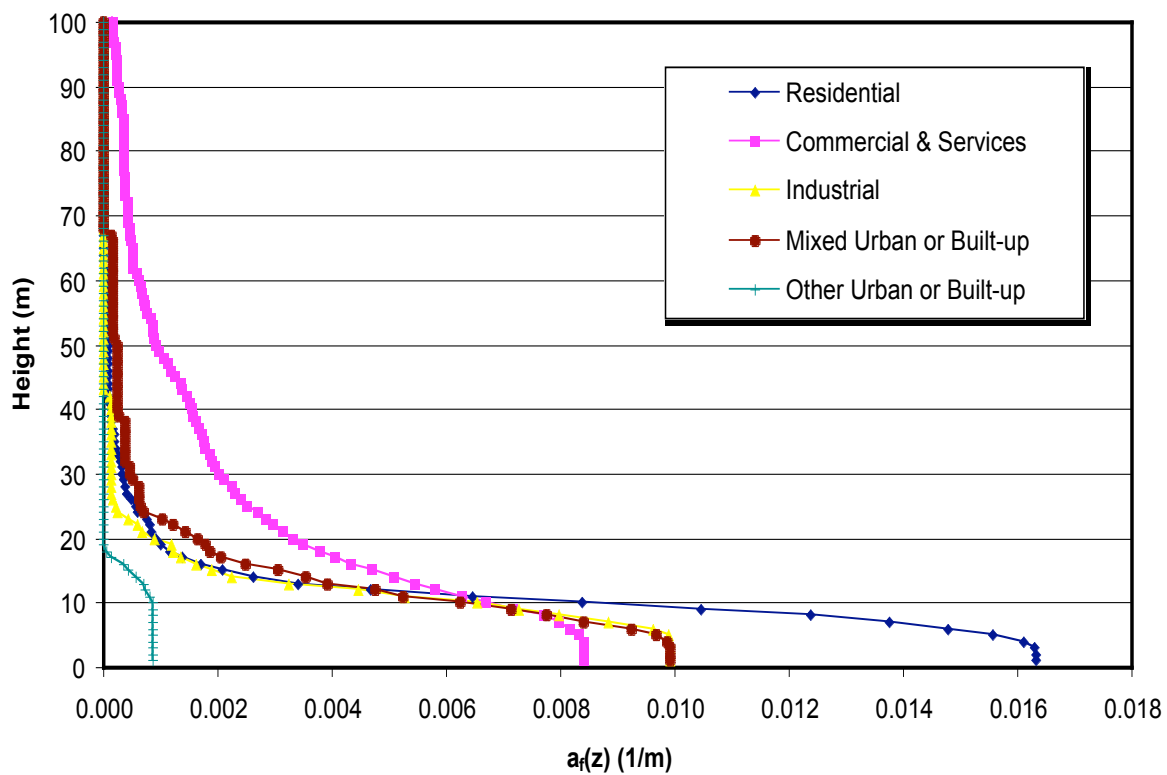


Figure 31. Frontal area density function ($a_f(z)$) for land use types in the 7-category scheme for a wind approaching from the north.

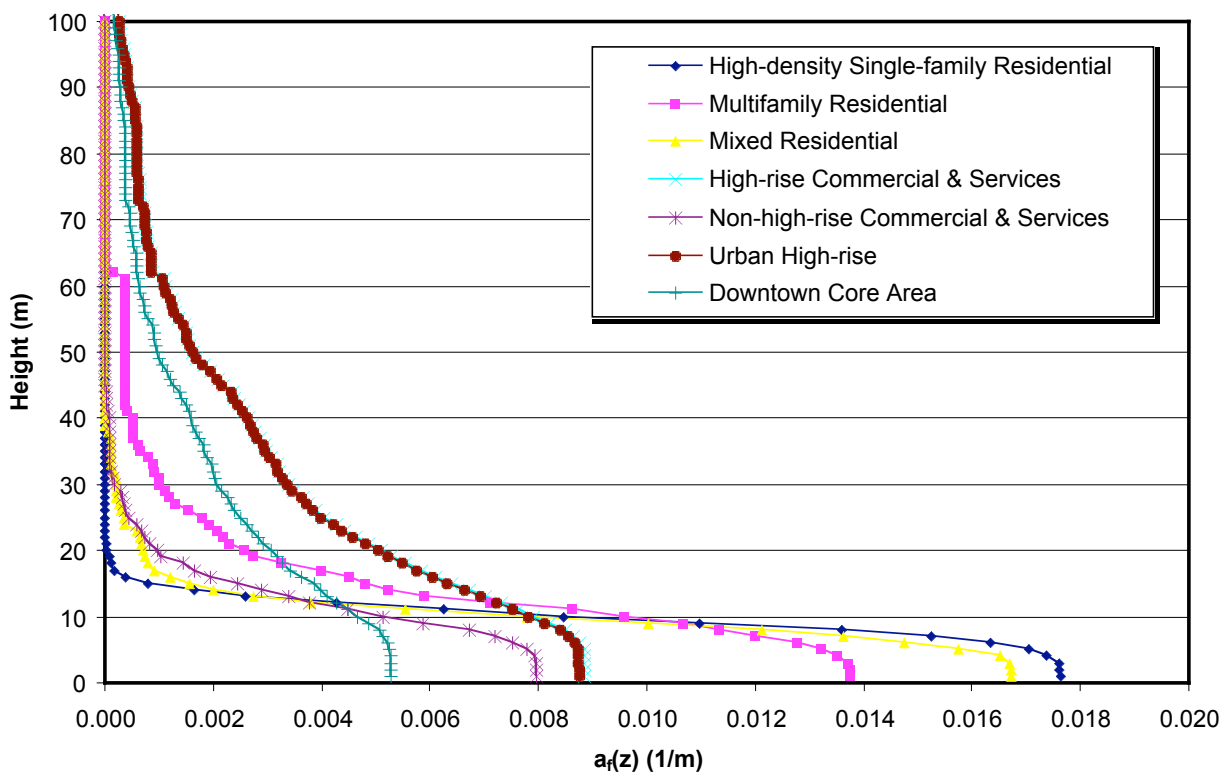


Figure 32. Frontal area density function ($a_f(z)$) for several land use types in the 12-category scheme and the Urban High-rise and Downtown Core Area land uses for a wind approaching from the north.

4.7 Complete Aspect Ratio (\square_C)

Background. The “complete” surface area, including building walls, roofs, and ground surfaces, is important when evaluating the urban canopy energy budget in a city. All of these surfaces act as sources and sinks of heat and need to be accounted for when evaluating the energy balance of an urbanized area. The non-dimensional form of the complete surface area, the complete aspect ratio, is useful in interpreting surface temperatures derived from remote sensing instruments. Used with the plan area \square_p , some notion of the three-dimensionality of the urban fabric can be obtained and better estimates of the “real” skin temperature might be computed.

Calculation Methods. The complete aspect ratio (\square_C) is defined as the summed surface area of roughness elements and exposed ground divided by the total plan area (Voogt and Oke 1997):

$$\square_C = \frac{A_C}{A_T} = \frac{A_W + A_R + A_G}{A_T} \quad (15)$$

where A_C is the combined surface area of the buildings and exposed ground, A_W is the wall surface area, A_R is the roof area, A_G is the area of exposed ground, and A_T is the plan area of the study site. A_C is calculated by summing the surface area of the buildings and the difference between the total plan area of the site and the plan area of buildings at ground level (i.e., the exposed ground surface). For dense urban areas with flat roofed buildings and without much vegetation, A_C can be approximated as the sum of the plan area of the site and the area of building walls (not including rooftops).

Using an Avenue script in the ArcView GIS we automatically calculated \square_C for the entire city for a non-uniform grid cell mesh (shown in Figure 20) and as a function of land use. Calculations were not possible for the uniform 100-m X 100-m mesh for the same reasons described for frontal area index. The rooftop surface area was calculated assuming the rooftops were flat, which a digital orthophoto indicated to be true for most of the land use types, except for some of the High-density Single-family Residential areas. Another source of error in our complete aspect ratio calculation is the neglect of the surface area of trees and bushes. Grimmond and Oke (1999) found the surface area of trees and bushes to be an important component of the complete surface area, especially in residential areas.

Results. For the 6.1-km² study area, the \square_C was calculated to be 1.70. The \square_C for each grid cell was calculated for the non-uniform grid cell mesh (Figure 33). For the non-uniform mesh, the mean \square_C was 1.70, with a standard deviation of 0.42, and a range of 1.05 to 4.71. The high-rise area is located within the conglomeration of red grid cells in Figure 33. The computed \square_C values for each land use type in our classification schemes are shown in Table 9. The \square_C values for the downtown area are in the range of 1.22 to 4.75, which are consistent with the central city values from other studies shown in Table 10.

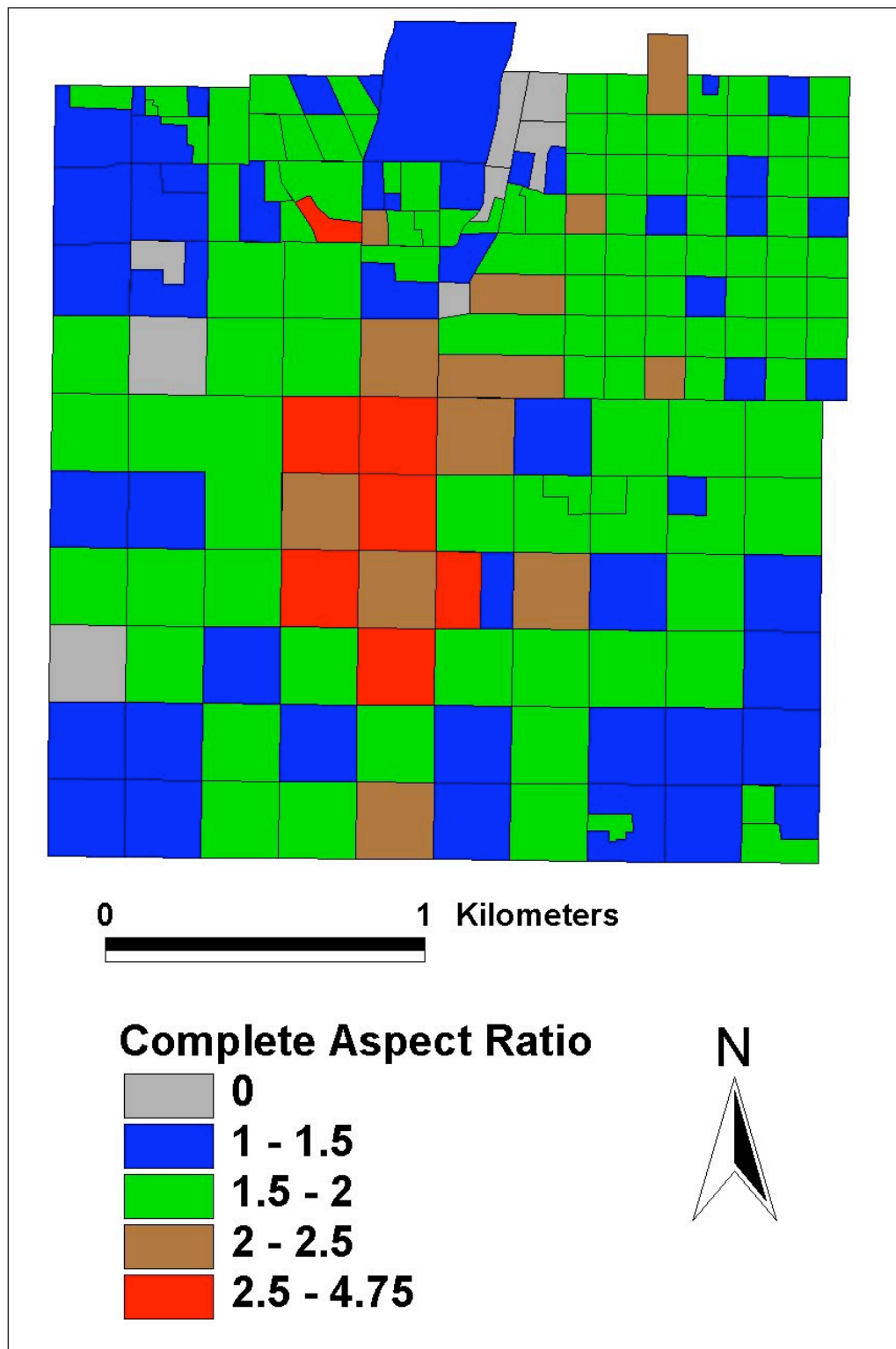


Figure 33. Display of complete aspect ratio (L_c) calculated for the Salt Lake City downtown area per grid cell.

Table 9. Complete aspect ratio ($\overline{\lambda}_c$) for each land use type

Land Use Class	$\overline{\lambda}_c$
Residential	1.70
Low-density Single-family (< 8 units/hectare)	---
High-density Single-family (\geq 8 units/hectare)	1.65
Multifamily	1.89
Mixed	1.63
Commercial & Services	1.79
Non-high-rise	1.42
High-rise	2.04
Industrial	1.48
Transportation/Communications/Utilities	---
Mixed Industrial & Commercial	---
Mixed Urban or Built-up	1.55
Other Urban or Built-up	1.05
Predominantly Vegetated	1.01
Predominantly Built-up	1.24
Urban High-rise	2.05
Downtown Core Area	1.64

Table 10 compares selected values from Table 9 with $\overline{\lambda}_c$ values computed for other cities. The $\overline{\lambda}_c$ computed for Salt Lake City Residential land use is in the upper half of the range found for other cities. The $\overline{\lambda}_c$ computed for the Industrial land use type in the Salt Lake City study area is greater than the value computed for a light industrial area in Vancouver. The downtown high-rise land use types in Salt Lake City have lower $\overline{\lambda}_c$ values compared to values computed for most other cities.

Table 10. Complete aspect ratio (\overline{L}_c) for downtown Salt Lake City and other cities

Location	Land Use Class	\overline{L}_c	Source
Salt Lake City, UT	Multifamily residential	1.89	This report
Arcadia, CA	Suburban residential	1.78	Grimmond and Oke (1999)
Los Angeles, CA	Multifamily residential	1.77	Burian et al. (2002b)
Chicago, IL	Suburban residential	1.74	Grimmond and Oke (1999)
Vancouver, BC, Canada	Suburban residential	1.65	Voogt and Oke (1997)
Salt Lake City, UT	High-density single-family residential	1.65	This report
Sacramento, CA	Suburban residential	1.63	Grimmond and Oke (1999)
Chicago, IL	Suburban residential	1.51	Grimmond and Oke (1999)
Tucson, AZ	Suburban residential	1.45	Grimmond and Oke (1999)
Miami, FL	Suburban residential	1.37	Grimmond and Oke (1999)
Los Angeles, CA	High-density single-family residential	1.36	Burian et al. (2002b)
San Gabriel, CA	Suburban residential	1.31	Grimmond and Oke (1999)
Salt Lake City, UT	Industrial	1.48	This report
Vancouver, BC, Canada	Light industrial	1.39	Voogt and Oke (1997)
Los Angeles, CA	Industrial	1.30	Burian et al. (2002b)
Los Angeles, CA	High-rise commercial & services	2.60	Burian et al. (2002b)
Los Angeles, CA	Urban high-rise	2.44	Burian et al. (2002b)
Los Angeles, CA	Downtown core area	2.22	Burian et al. (2002b)
Vancouver, BC, Canada	Central city	2.20	Voogt and Oke (1997)
Salt Lake City, UT	Urban high-rise	2.05	This report
Mexico City, Mexico	Central city	1.73	Grimmond and Oke (1999)
Singapore	Downtown	1.70	Nichol (1996)

4.8 Building Surface Area to Plan Area Ratio (\square_B)

Background. Another measure of urban terrain character is the ratio of built surface area to the plan surface area. Like the complete aspect ratio (Section 4.7), the building surface area is important when evaluating the urban canopy energy budget in a city. Building walls and roof surfaces act as sources and sinks of heat and need to be accounted for when evaluating the energy balance of an urbanized area. Perhaps some combination of frontal area, plan area, complete surface area, and building surface area parameters will allow for better parameterizations of the urban canopy energy budget.

Calculation Methods. The building surface area to plan area ratio (\square_B) is defined as the sum of building surface area divided by the total plan area:

$$\square_B = \frac{A_R + A_W}{A_T} \quad (16)$$

where A_R is the plan area of rooftops, A_W is the total area of non-horizontal roughness element surfaces (e.g., walls), and A_T is the total plan area of the study location. For the calculations below, we have made a flat-roof assumption.

Results. The \square_B for the 6.1-km² study area in Salt Lake City was calculated to be 0.94. Table 11 shows the computed \square_B values for each land use type included in the building analysis. Commercial & Services High-rise, Urban High-rise, and Downtown Core Area have the largest values due to the presence of tall buildings and fairly high plan area fraction. We did not find values for other cities for this parameter.

Table 11. Building surface area to plan area ratio (\square_B) for each land use type

Land Use Class	\square_B
Residential	0.91
Low-density Single-family (< 8 units/hectare)	---
High-density Single-family (\geq 8 units/hectare)	0.84
Multifamily	1.15
Mixed	0.84
Commercial & Services	1.07
Non-high-rise	0.63
High-rise	1.37
Industrial	0.74
Transportation/Communications/Utilities	---
Mixed Industrial & Commercial	---
Mixed Urban or Built-up	0.76
Other Urban or Built-up	0.07
Predominantly Vegetated	0.02
Predominantly Built-up	0.32
Urban High-rise	1.38
Downtown Core Area	0.84

4.9 Height-to-Width Ratio ($\bar{\lambda}_s$)

Background. The ratio of the height of buildings to the horizontal distance (or street width) between the buildings is called the height-to-width ratio ($\bar{\lambda}_s$). The height-to-width ratio has been found, for idealized arrangements of same-height buildings, to influence the flow regime. Hussain and Lee (1980) performed wind-tunnel experiments and found the three flow regimes develop in idealized urban street canyons: (1) isolated flow, (2) wake interference flow, and (3) skimming flow. The isolated flow regime occurs when elements are spaced relatively far apart ($\bar{\lambda}_s < 0.4$), the wake interference flow occurs when elements are spaced at a medium density level ($0.4 < \bar{\lambda}_s < 0.7$), and the skimming flow regime occurs for high-density building arrangements ($\bar{\lambda}_s > 0.7$) (Oke 1988).

Calculation Methods. The height-to-width ratio ($\bar{\lambda}_s$) (also called the street aspect ratio) is calculated for two buildings by dividing the average height by the distance between the two buildings:

$$\bar{\lambda}_s = \frac{(H_1 + H_2)/2}{S_{12}} \quad (17)$$

where H_1 is the height of the upwind building, H_2 is the height of the downwind building, and S_{12} is the horizontal distance between the two buildings (i.e., the canyon width). Figure 34 illustrates the measures used to compute $\bar{\lambda}_s$. The calculation of $\bar{\lambda}_s$ is performed for each pair of adjacent elements in a building array, which can be very tedious for the complex building shapes and patterns in a city. For idealized arrangements of buildings, the calculation of an average $\bar{\lambda}_s$ can be approximated by taking the average building height divided by the average width between buildings (Grimmond and Oke 1999):

$$\overline{\bar{\lambda}_s} \approx \frac{\overline{z_H}}{\overline{W}} \quad (18)$$

where $\overline{z_H}$ is the average building height and \overline{W} is the average distance between buildings.

Due to the large number of buildings in the Salt Lake City dataset, an automated approach is warranted. Because of the complexity of the Salt Lake City downtown area, we did not use the simplified methodology described by Eqn. (18). Instead, we computed $\bar{\lambda}_s$ along linear traverses across the city at different angles using Eqn. (17). Our calculation strategy involved converting the urban building database into a raster digital elevation model (DEM – a matrix of numbers representing building height). Then traversing along each row or column of grid cells the height-to-width ratio was calculated between each pair of buildings. A Fortran code was written to execute this procedure. Since this approach yields $\bar{\lambda}_s$ values in non-preferred directions (e.g., running along a street, not across a street), we then superimposed the matrices of traverses done at different angles, and chose the height-to-width ratio at each grid cell by selecting the largest value.

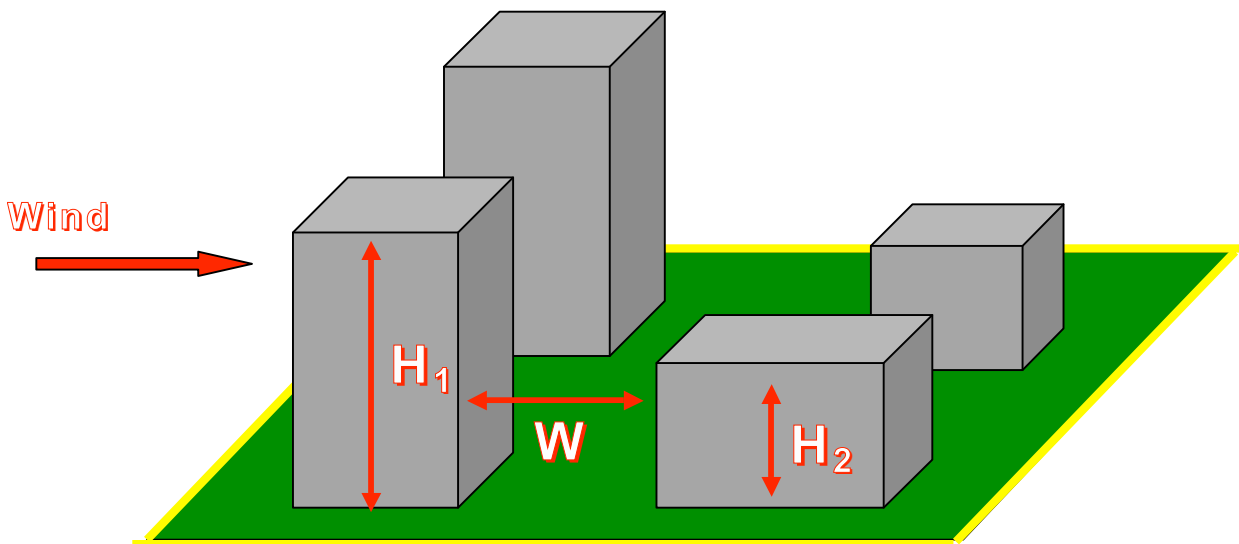


Figure 34. Illustration of height-to-width ratio parameter.

Figures 35 and 36 show the spatial distribution of the computed \bar{L}_s values for the two analysis directions that corresponded with the predominant street directions. Due to the unidirectional nature of the traverses, one can plainly see that the height-to-width ratio is too small between some buildings. For example, in Fig. 35 the \bar{L}_s values are underestimated along the south-to-north-running streets. Figure 37 shows the composite \bar{L}_s values, which were computed at each grid cell by selecting the largest value from the superimposed matrices from the two traversal directions, i.e., superimposing the values from Figs. 35 and 36. The higher \bar{L}_s values are clearly visible in the downtown area of Salt Lake City (the buildings are shaded by height).

Figures 38, 39, and 40 show the composite \bar{L}_s values for areas predominantly composed of Residential, Industrial, and Downtown Core Area land uses, respectively. The figures clearly illustrate the concentration of the highest \bar{L}_s values in the high-rise area. The \bar{L}_s values are fairly similar for the Residential and Industrial land uses.

We also computed the average \bar{L}_s values for the study area and for each land use type in our classification schemes. The average \bar{L}_s was computed by using the area-weighted average of the spatial distribution of the composite height-to-width ratio shown in Figure 37. One could also weight the average \bar{L}_s by number of buildings, streets, or some other quantity. In the approach used here, buildings with larger footprints will exert a greater influence over the area-weighted average. In addition, open areas (e.g., parking lots and parks) and street intersections will be counted in the average.

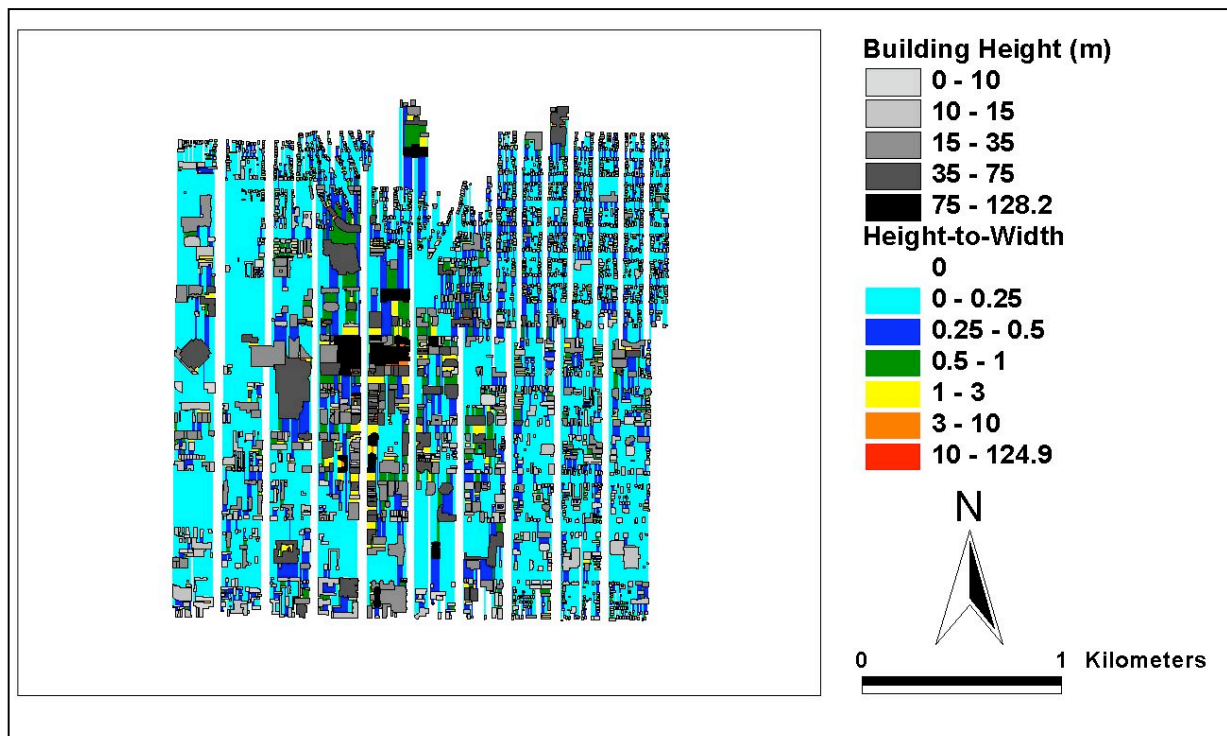


Figure 35. Computed height-to-width ratio (H_s) for the Salt Lake City study area (analysis traversal was from north to south).

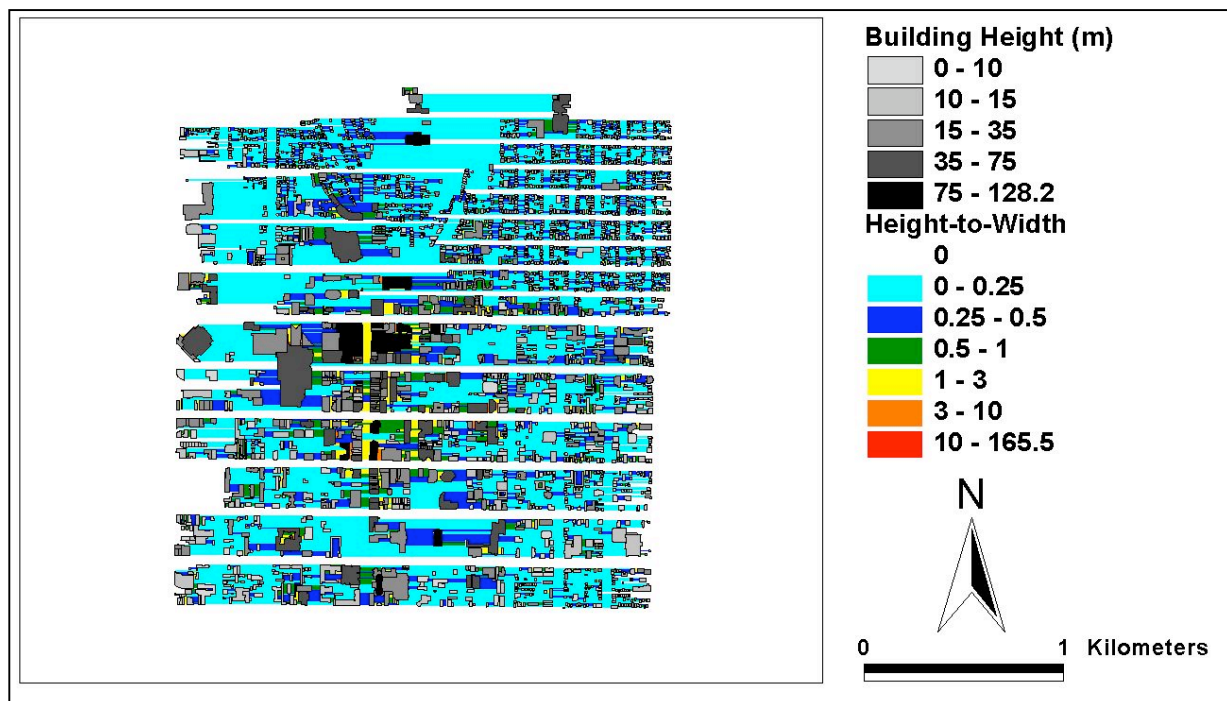


Figure 36. Computed height-to-width ratio (H_s) for the Salt Lake City study area (analysis traversal was from west to east).

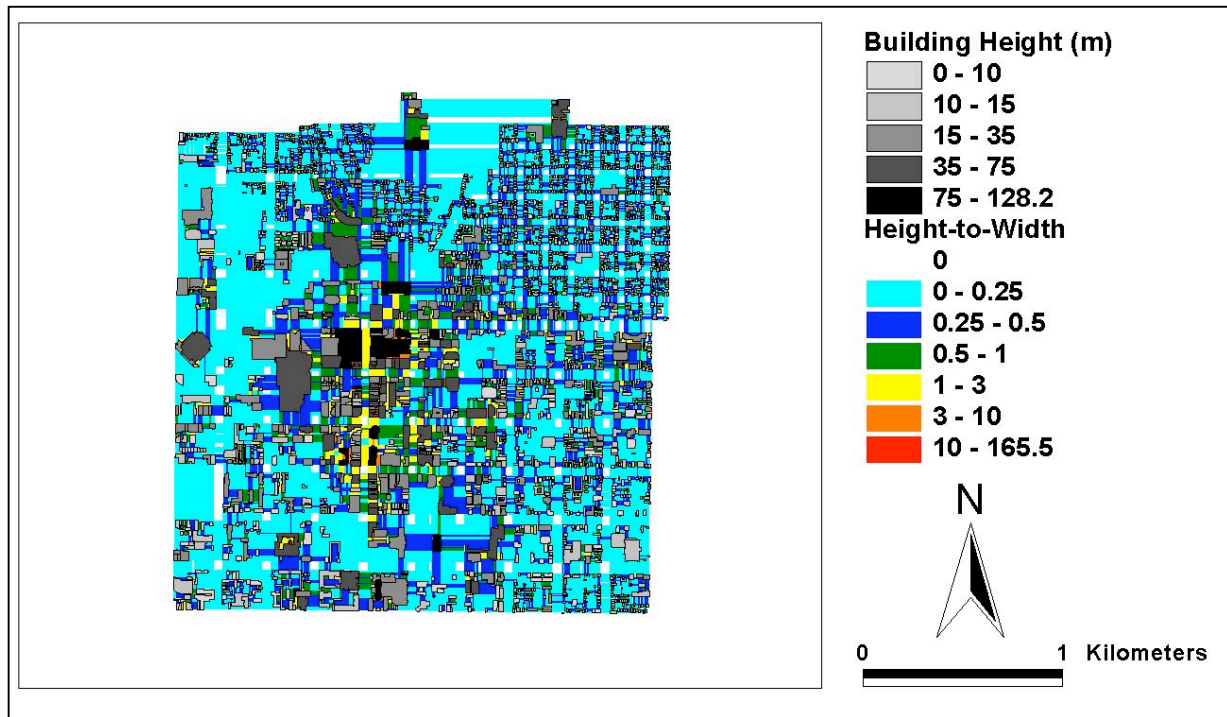


Figure 37. Composite height-to-width ratio ($\overline{h_s}$) for the Salt Lake City study area based on the integration of computed values for the two analysis traversals.

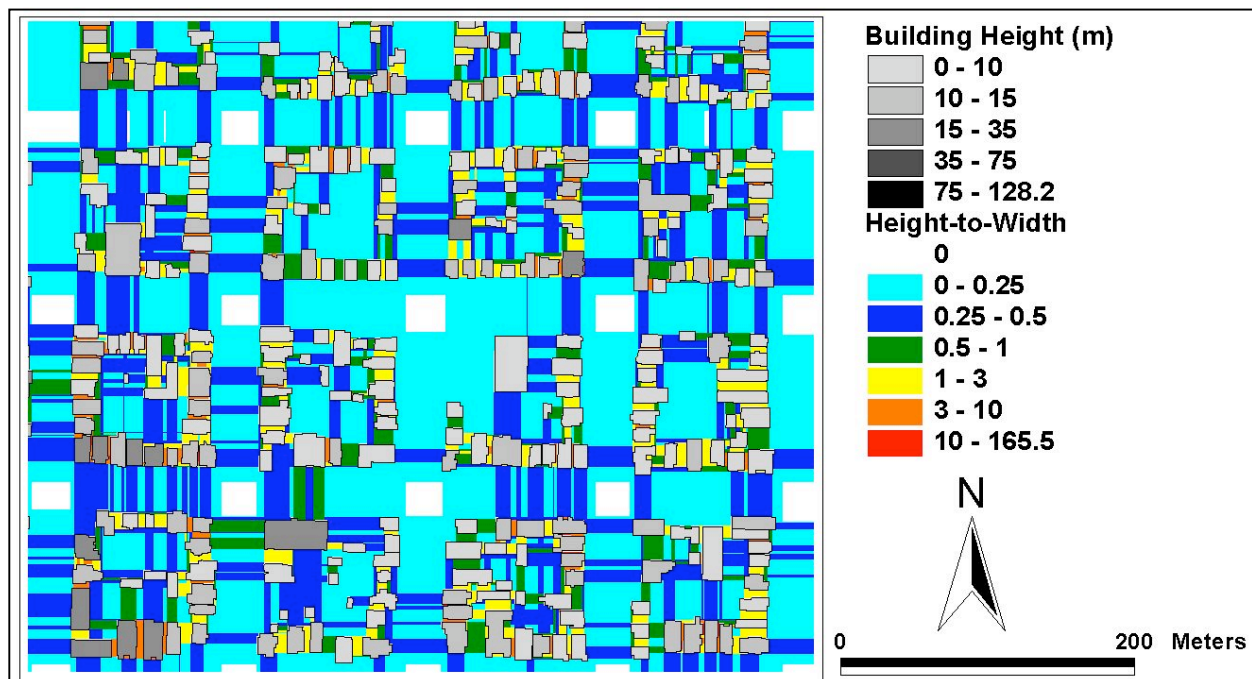


Figure 38. Composite height-to-width ratio ($\overline{h_s}$) for a Residential section of the Salt Lake City study area.

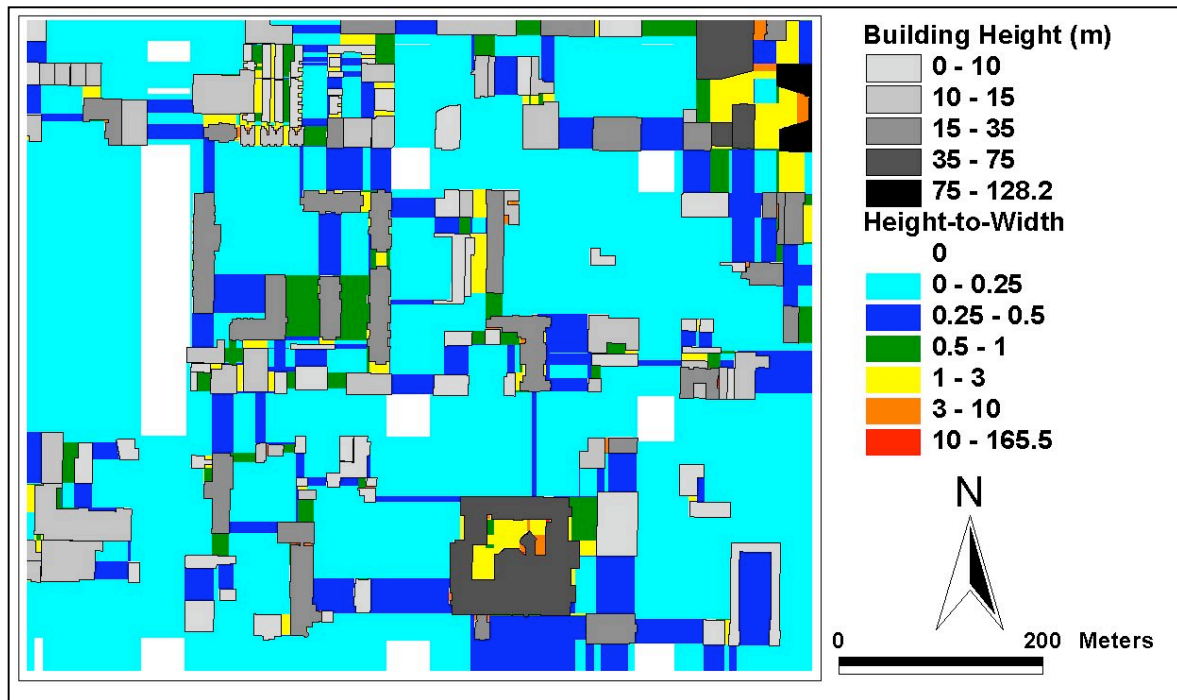


Figure 39. Composite height-to-width ratio (\overline{H}_s) for an Industrial section of the Salt Lake City study area.

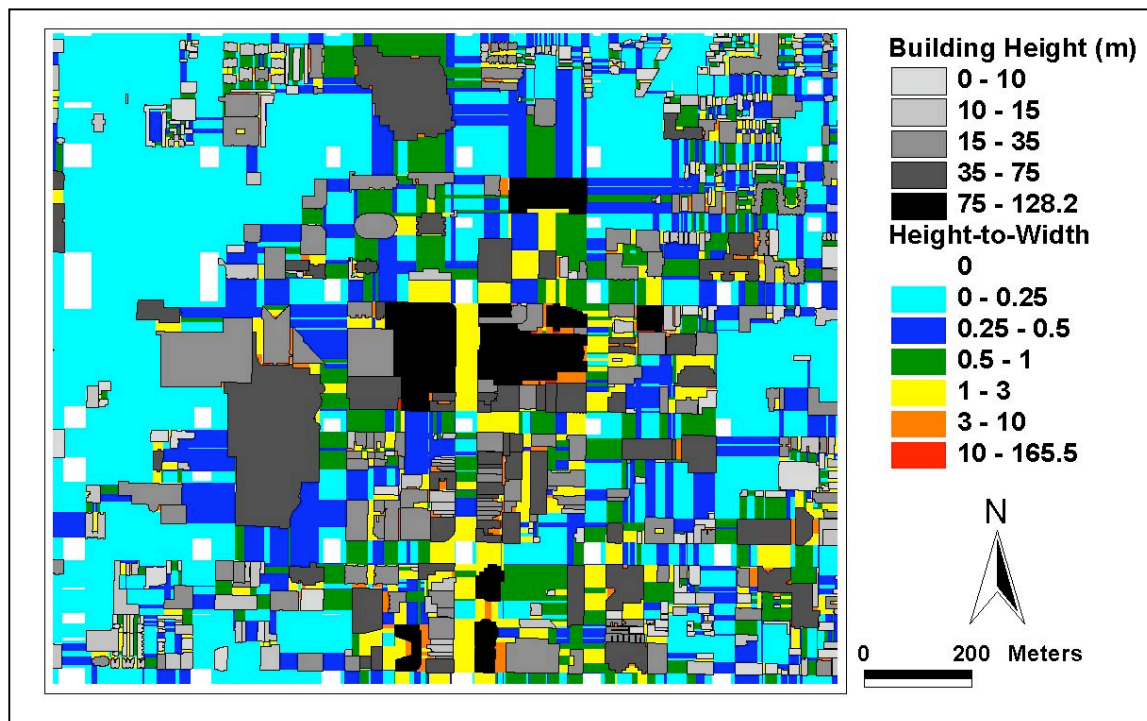


Figure 40. Composite height-to-width ratio (\overline{H}_s) for the Downtown Core Area of the Salt Lake City study area.

Results. The area-weighted average \overline{L}_s for the study area was calculated to be 0.34. The range of \overline{L}_s for the study area was 0 to 124.9. Zero values occur where buildings are located and in regions where two buildings do not lie on an ‘along-the-street’ or ‘across-the-street’ transect. Table 12 lists the area-weighted average \overline{L}_s values for each land use type.

Table 12. Area-weighted average composite height-to-width ratio (\overline{L}_s)

Land Use Class	\overline{L}_s
Residential	0.37
Low-density Single-family (< 8 units/hectare)	---
High-density Single-family (\geq 8 units/hectare)	0.34
Multifamily	0.47
Mixed	0.24
Commercial & Services	0.37
Non-high-rise	0.23
High-rise	0.49
Industrial	0.23
Transportation/Communications/Utilities	---
Mixed Industrial & Commercial	---
Mixed Urban or Built-up	0.31
Other Urban or Built-up	0.06
Predominantly Vegetated	0.05
Predominantly Built-up	0.14
Urban High-rise	0.50
Downtown Core Area	0.54

Table 13 compares selected values from our study with values computed for other cities. The values we calculated for Salt Lake City are on the lower end of the range of values from other cities. The much larger values computed in other studies for the Residential land use are possibly attributable to the inclusion of trees in the height-to-width calculations. Also, the downtown study area included significant amounts of parking lots, which reduced the composite height-to-width ratios. Finally, the averaging scheme could cause significant differences; sensitivity studies need to be performed.

Table 13. Comparison of height-to-width (L_s) for Salt Lake City and other cities

Location	Land Use Class	L_s	Source
Sacramento, CA	Suburban residential	1.21	Grimmond and Oke (1999)
Arcadia, CA	Suburban residential	1.19	Grimmond and Oke (1999)
Miami, FL	Suburban residential	1.03	Grimmond and Oke (1999)
Chicago, IL	Suburban residential	0.97	Grimmond and Oke (1999)
Vancouver, BC, Canada	Suburban residential	0.90	Grimmond and Oke (1999)
Tucson, AZ	Suburban residential	0.54	Grimmond and Oke (1999)
Salt Lake City, UT	Multifamily residential	0.47	This report
Los Angeles, CA	Multifamily residential	0.45	Burian et al. (2002b)
San Gabriel, CA	Suburban residential	0.43	Grimmond and Oke (1999)
Los Angeles, CA	High-density single-family residential	0.23	Burian et al. (2002b)
Vancouver, BC, Canada	Light industrial	0.57	Grimmond and Oke (1999)
Salt Lake City, UT	Industrial	0.23	This report
Los Angeles, CA	Industrial	0.20	Burian et al. (2002b)
Vancouver, BC, Canada	Central city	1.40	Grimmond and Oke (1999)
Mexico City, Mexico	Central city	1.19	Grimmond and Oke (1999)
Los Angeles, CA	Commercial & services high-rise	0.91	Burian et al. (2002b)
Los Angeles, CA	Downtown core area	0.77	Burian et al. (2002b)
Salt Lake City, UT	Downtown core area	0.54	This report

4.10 Aerodynamic Roughness Parameters

Background. The representation of surface roughness is a critical first step in many meteorological, wind engineering, and pollutant dispersion modeling activities. It provides an estimate of the drag and turbulent mixing associated with the underlying surface. The displacement height (z_d) and roughness length (z_o) are key parameters in the logarithmic velocity profile based on similarity theory and is commonly used in many models to specify the boundary conditions above built-up areas. The displacement height can be conceptualized as the height of a surface formed by distributing the aggregate volume of roughness elements and their wake recirculation cavities uniformly over the underlying surface (Macdonald et al. 1998). The roughness length is directly related to the overall drag of the surface. Mathematically, it represents the distance above the displacement height plane at which the velocity goes to zero.

Both z_d and z_o are difficult to estimate with certainty by experiment or theory. Grimmond and Oke (1999) reviewed methods to calculate the z_d and z_o of urban areas based on building and vegetation morphology. They compared the predictions of the morphological methods to those obtained from wind measurements in urban areas. Using the equations rated amongst the most appropriate by Grimmond and Oke (1999), we calculated values of z_d and z_o for the entire Salt Lake City study area, spatially over a defined grid and as a function of land use in the study area. Note that the similarity theory is not valid in horizontally inhomogeneous areas and that for many urban areas the roughness parameter concept will not hold or can only be applied well above the roughness elements.

Calculation Methods. A common method used to calculate the displacement height (z_d) and roughness length (z_o) are simple rules-of-thumb (Grimmond and Oke 1999):

$$z_d = f_d \overline{z_H} \quad (19)$$

and

$$z_o = f_o \overline{z_H} \quad (20)$$

where $\overline{z_H}$ is the average building height and f_d and f_o are empirical coefficients. Approximations for urban values are 0.5 for f_d and 0.1 for f_o . Beyond the limitations of applying these equations to horizontally inhomogeneous urban areas, these equations also only hold for medium building density situations, as it is known that z_o and z_d vary with building spacing.

Results. Although Eqns. (19) and (20) may not hold for all areas in our study domain, we have still computed the aerodynamic roughness parameters for the Salt Lake City study area for comparison purposes. Using these approximations we found that $z_d \approx 6.00$ m and $z_o \approx 1.20$ m when using the mean building height, and $z_d \approx 12.75$ m and $z_o \approx 2.55$ m when using the plan-area-weighted average building height. Table 14 lists the computed z_d and z_o values for each land use type using the mean building height and Eqns. (19) and (20). Table 15 lists the computed z_d and z_o values for each land use type using the plan-area-weighted average building height and Eqns. (19) and (20), while Figures 41 and 42 show the spatial distribution of the z_d and z_o .

Table 14. Displacement height (z_d) and roughness length (z_o): simple rules-of-thumb eqns. and average building height.

Land Use Class	z_d (m)	z_o (m)
Residential	4.80	0.96
Low-density Single-family (< 8 units/hectare)	---	---
High-density Single-family (\geq 8 units/hectare)	4.65	0.93
Multifamily	5.50	1.10
Mixed	4.55	0.91
Commercial & Services	8.95	1.79
Non-high-rise	5.75	1.15
High-rise	11.70	2.34
Industrial	5.40	1.08
Transportation/Communications/Utilities	---	---
Mixed Industrial & Commercial	---	---
Mixed Urban or Built-up	5.60	1.12
Other Urban or Built-up	6.90	1.38
Predominantly Vegetated	5.70	1.14
Predominantly Built-up	7.90	1.58
Urban High-rise	11.75	2.35
Downtown Core Area	11.80	2.36

Table 15. Displacement height (z_d) and roughness length (z_o): simple rules-of-thumb eqns. and plan-area-weighted average building height.

Land Use Class	z_d (m)	z_o (m)
Residential	6.65	1.33
Low-density Single-family (< 8 units/hectare)	---	---
High-density Single-family (\geq 8 units/hectare)	4.95	0.99
Multifamily	8.30	1.66
Mixed	5.60	1.12
Commercial & Services	14.45	2.89
Non-high-rise	7.65	1.53
High-rise	20.20	4.04
Industrial	6.40	1.28
Transportation/Communications/Utilities	---	---
Mixed Industrial & Commercial	---	---
Mixed Urban or Built-up	7.70	1.54
Other Urban or Built-up	7.50	1.50
Predominantly Vegetated	6.20	1.24
Predominantly Built-up	7.90	1.57
Urban High-rise	11.75	4.05
Downtown Core Area	11.80	4.15

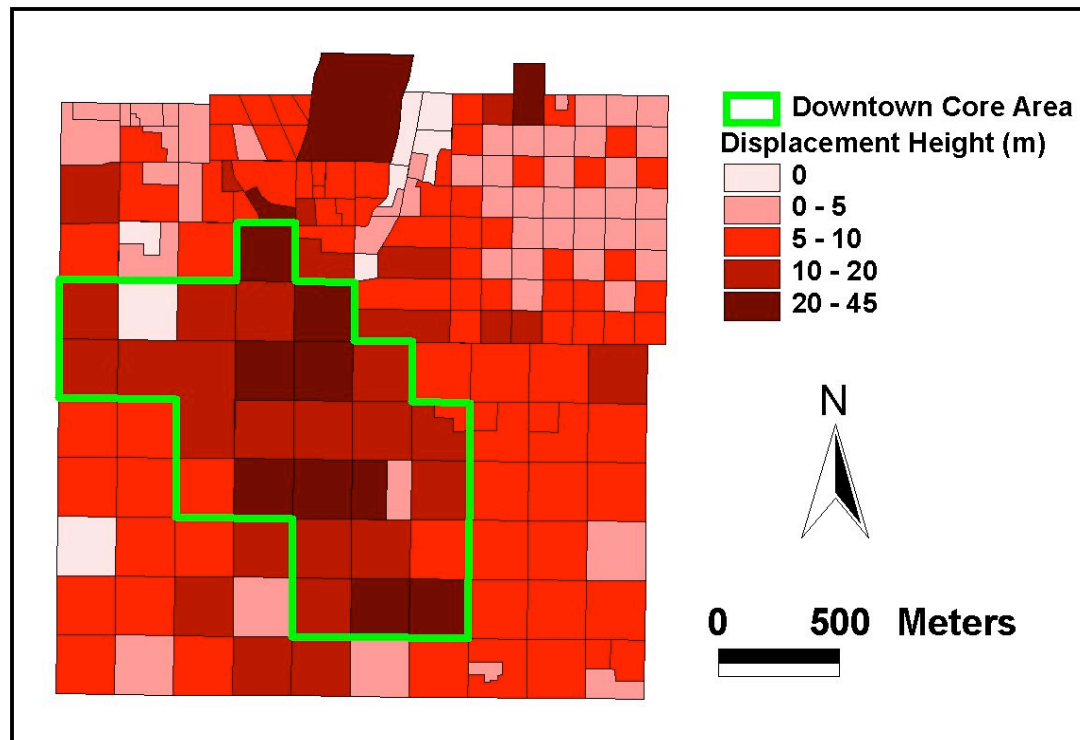


Figure 41. Spatial distribution of displacement height (z_d) in downtown Salt Lake City computed using the simple rule-of-thumb (Eqn. (19)) and the plan-area-weighted average building height.

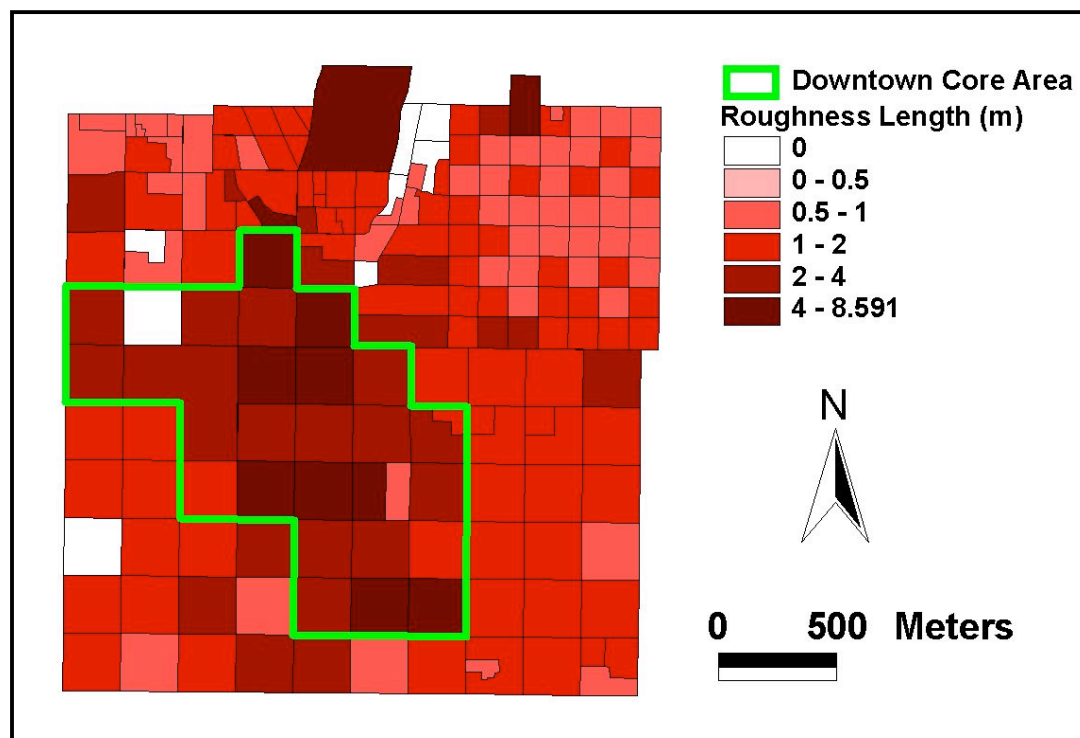


Figure 42. Spatial distribution of the roughness length (z_o) in downtown Salt Lake City computed using the simple rule-of-thumb (Eqn. 20) and the plan area-weighted average building height.

Calculation Methods. We also computed the z_d and z_o using two more complex equations described by Grimmond and Oke (1999). Although they compared results produced by different equations and concluded that it is difficult to measure their predictive accuracy, they did suggest an ordering of the morphometric equations. One set of equations ranked highly were those by Raupach (1994):

$$\frac{z_d}{z_H} = 1 - \frac{\exp[-(c_{d1} 2\bar{\Delta}_f)^{0.5}]}{(c_{d1} 2\bar{\Delta}_f)^{0.5}} \quad (21)$$

and

$$\frac{z_o}{z_H} = \frac{z_d}{z_H} \exp\left[-k \frac{U}{u_\square}\right] + \Delta_k \quad (22)$$

where

$$\frac{u_\square}{U} = \min\left[(c_S + c_R \bar{\Delta}_f)^{0.5}, \frac{u_\square}{U_{\max}}\right] \quad (23)$$

and Δ_k is the roughness sublayer influence function, U and u_* are the large-scale wind speed and the friction velocity, respectively, c_S and c_R are drag coefficients for the substrate surface at height z_H in the absence of roughness elements and of an isolated roughness element mounted on the surface, respectively, and c_{d1} is a free parameter. Raupach (1994) suggested $\Delta_k = 0.193$, $(u_*/U)_{\max} = 0.3$, $c_S = 0.003$, $c_R = 0.3$, and $c_{d1} = 7.5$.

Results. Using these values, a von Kármán constant (k) of 0.4, and the values computed for the average building height and the average frontal area index, we calculated $z_d = 6.38$ m and $z_o = 1.43$ m. When using the plan-area-weighted average building height we found $z_d = 13.51$ m and $z_o = 3.03$ m. These values are very similar to those derived using the simple scheme described above (Eqns. (19) and (20)). Tables 16 and 17 list the computed z_d and z_o for each land use type using the average building height and the plan-area-weighted average building height, respectively.

Table 16. Displacement height (z_d) and roughness length (z_o):
Raupach (1994) equations with the average building height

Land Use Class	z_d (m)	z_o (m)
Residential	5.08	1.14
Low-density Single-family (< 8 units/hectare)	---	---
High-density Single-family (\geq 8 units/hectare)	4.87	1.08
Multifamily	6.13	1.41
Mixed	4.72	1.04
Commercial & Services	9.82	2.24
Non-high-rise	5.17	1.02
High-rise	13.90	3.04
Industrial	5.15	1.07
Transportation/Communications/Utilities	---	---
Mixed Industrial & Commercial	---	---
Mixed Urban or Built-up	5.49	1.17
Other Urban or Built-up	2.77	0.13
Predominantly Vegetated	1.28	0.03
Predominantly Built-up	6.00	0.94
Urban High-rise	13.93	3.06
Downtown Core Area	12.25	2.72

Table 17. Displacement height (z_d) and roughness length (z_o):
Raupach (1994) equations with the plan-area-weighted

Land Use Class	z_d (m)	z_o (m)
Residential	7.04	1.58
Low-density Single-family (< 8 units/hectare)	---	---
High-density Single-family (\geq 8 units/hectare)	5.18	1.15
Multifamily	9.26	2.12
Mixed	5.80	1.29
Commercial & Services	15.85	3.61
Non-high-rise	6.88	1.35
High-rise	24.00	5.24
Industrial	6.10	1.27
Transportation/Communications/Utilities	---	---
Mixed Industrial & Commercial	---	---
Mixed Urban or Built-up	7.55	1.60
Other Urban or Built-up	3.01	0.14
Predominantly Vegetated	1.40	0.03
Predominantly Built-up	5.97	0.94
Urban High-rise	24.00	5.27
Downtown Core Area	21.54	4.78

Calculation Methods. The second set of equations was derived by Macdonald et al. (1998). These equations incorporate the drag coefficient and displacement height into the expression for roughness length (z_o):

$$\frac{z_d}{z_H} = 1 + \alpha_p (\alpha_p - 1) \quad (24)$$

and

$$\frac{z_o}{z_H} = \left(\frac{z_d}{z_H} \right) \exp \left(-0.5 \alpha_p \frac{C_D}{k^2} \left(\frac{z_d}{z_H} \right)^f \right)^{0.5} \quad (25)$$

where α is an empirical coefficient, C_D is a drag coefficient, k is the von Kármán constant, and f is a correction factor for the drag coefficient (the net correction for several variables, including velocity profile shape, incident turbulence intensity, turbulence length scale, and incident wind angle, and for rounded corners). Macdonald et al. (1998) recommended for staggered arrays of cubes that $\alpha = 4.43$ and $f = 1.0$. These values were used by Grimmond and Oke (1999) and are also used here. We also set $C_D = 1.2$ (the same value used Grimmond and Oke (1999) in their analysis) and the von Kármán constant $k = 0.4$.

Results. We found $z_d = 5.46$ m and $z_o = 1.42$ m for the Salt Lake City study area. Using the plan-area-weighted average building height we found $z_d = 11.56$ m and $z_o = 3.00$ m. This method gives approximately the same value for z_o compared to the values computed using the Raupach (1994) equations and slightly smaller z_d values. Tables 18 and 19 list the computed z_d and z_o for each land use for the average building height and the plan-area-weighted average building height, respectively.

Table 20 compares the computed aerodynamic roughness parameters to those calculated for other cities. The roughness parameters shown in Table 20 for Salt Lake City were calculated using the Raupach (1994) equations with the plan-area-weighted average building height. The values for Salt Lake City are comparable to values from other locations. The Multifamily Residential land use in Salt Lake City has similar displacement and roughness lengths as the Multifamily Residential land use in Los Angeles. The displacement and roughness lengths for Industrial land use in Salt Lake City are slightly larger than values found for Industrial land use in other cities. The values for the Downtown Core Area are in the middle of the range of values found for other cities. The computed roughness length of 1.15 m for the tract of High-density Single-family Residential using the Raupach (1994) equations is beyond the range of 0.4-0.7 m presented by Wieringa (1993) for homogeneous suburban low buildings.

Table 18. Displacement height (z_d) and roughness length (z_o):
Macdonald et al. (1998) equations with the average building height

Land Use Class	z_d (m)	z_o (m)
Residential	4.05	1.24
Low-density Single-family (< 8 units/hectare)	---	---
High-density Single-family (\geq 8 units/hectare)	3.62	1.29
Multifamily	5.30	1.36
Mixed	3.84	1.11
Commercial & Services	9.16	1.90
Non-high-rise	4.67	0.99
High-rise	13.81	2.30
Industrial	5.53	0.76
Transportation/Communications/Utilities	---	---
Mixed Industrial & Commercial	---	---
Mixed Urban or Built-up	4.36	1.30
Other Urban or Built-up	0.67	0.16
Predominantly Vegetated	0.28	0.00
Predominantly Built-up	3.23	1.48
Urban High-rise	13.87	2.29
Downtown Core Area	13.92	1.54

Table 19. Displacement height (z_d) and roughness length (z_o):
Macdonald et al. (1998) equations with the plan-area-weighted average building height

Land Use Class	z_d (m)	z_o (m)
Residential	5.61	1.72
Low-density Single-family (< 8 units/hectare)	---	---
High-density Single-family (\geq 8 units/hectare)	3.86	1.37
Multifamily	8.00	2.05
Mixed	4.73	1.37
Commercial & Services	14.79	3.07
Non-high-rise	6.21	1.32
High-rise	23.84	3.97
Industrial	6.55	0.90
Transportation/Communications/Utilities	---	---
Mixed Industrial & Commercial	---	---
Mixed Urban or Built-up	6.00	1.79
Other Urban or Built-up	0.73	0.18
Predominantly Vegetated	0.31	0.00
Predominantly Built-up	3.20	1.47
Urban High-rise	23.90	3.95
Downtown Core Area	24.49	2.71

Table 20. Displacement height (z_d) and roughness length (z_o) for different cities

Location	Land Use Class	z_d (m)	z_o (m)	Source
Salt Lake City, UT	Multifamily residential	9.26	2.12	This report*
Los Angeles, CA	Multifamily residential	9.24	2.12	Burian et al. (2002b)*
Arcadia, CA	Suburban residential	6.75	1.50	Grimmond and Oke (1999), Fig. 4
Salt Lake City, UT	High-density single-family residential	5.18	1.15	This report*
Vancouver, BC, Canada	Suburban residential	4.10	0.95	Grimmond and Oke (1999), Fig. 4
Chicago, IL	Suburban residential	4.00	0.75	Grimmond and Oke (1999), Fig. 4
Miami, FL	Suburban residential	3.25	0.80	Grimmond and Oke (1999), Fig. 4
Sacramento, CA	Suburban residential	3.10	0.75	Grimmond and Oke (1999), Fig. 4
San Gabriel, CA	Suburban residential	2.35	0.6	Grimmond and Oke (1999), Fig. 4
Los Angeles, CA	High-density single-family residential	2.24	0.44	Burian et al. (2002b)*
Tucson, AZ	Suburban residential	2.10	0.40	Grimmond and Oke (1999), Fig. 4
Salt Lake City, UT	Industrial	6.10	1.27	This report*
Vancouver, BC, Canada	Light industrial	2.25	0.5	Grimmond and Oke (1999), Fig. 4
Los Angeles, CA	Industrial	3.04	0.54	Burian et al. (2002b)*
Los Angeles, CA	Commercial & services high-rise	32.11	5.31	Burian et al. (2002b)*
Los Angeles, CA	Downtown core area	27.38	535	Burian et al. (2002b)*
Salt Lake City, UT	Downtown core area	21.54	4.78	This report*
Vancouver, BC, Canada	Central city	20.00	4.50	Grimmond and Oke (1999), Fig. 4
Mexico City, Mexico	Central city	8.00	1.60	Grimmond and Oke (1999), Fig. 4

* SLC and LA values computed using the Raupach (1994) equations and the plan-area-weighted building height

5.0 Summary

This report summarizes the results of the derivation of building morphological characteristics for a 6.1 km² area of downtown Salt Lake City, Utah. A three-dimensional building dataset and detailed land use/land cover information were integrated and analyzed using a geographic information system (GIS). Building height characteristics (e.g., mean height, height variance, height histograms) were determined for the entire study area and broken down by land use type. Parameters describing the urban morphology were also calculated including the building plan area fraction ($\overline{f_p}$), building area density ($a_p(z)$), rooftop area density ($a_r(z)$), frontal area index ($\overline{f_f}$), frontal area density ($a_f(z)$), complete aspect ratio ($\overline{f_c}$), building surface area to plan area ratio ($\overline{f_B}$), and the height-to-width ratio ($\overline{f_s}$). These urban morphological parameters were calculated for the entire study area, for different land use types, and in some cases as a function of height above ground elevation. Using the urban morphological parameters, the aerodynamic roughness length (z_o) and displacement height (z_d) were calculated for the entire study area and for each land use type using standard morphometric equations. Most of the calculated morphometric parameters were found to be similar to values computed for other cities by other researchers. Synthesis of the results indicates that the urban morphological parameters vary significantly between different land uses. Moreover, the urban land uses containing tall buildings were found to have significantly different morphological characteristics than other urban land uses.

References

- Anderson, J. R., Hardy, E. E., Roach, J. T. and Witmer, R. E. (1976). *A land use and land cover classification system for use with remote sensor data*. USGS Professional Paper 964, U.S. Geological Survey.
- Brown, M.J. (1999). *Urban parameterizations for mesoscale meteorological models*. Mesoscale Atmospheric Dispersion, Edited by Z. Boybeyi, WIT Press, pp. 193-255, LA-UR-99-5329.
- Burian, S.J. and Brown, M.J. (2001). *Summary of Los Angeles, California urban building and land use/cover data*. LA-UR-01-4055, Los Alamos National Laboratory, Los Alamos, New Mexico.
- Burian, S.J., Brown, M.J., and Velugubantla, S.P. (2002a). "Building height characteristics in three U.S. cities." *Preprints, Fourth Symposium on the Urban Environment*, 20-24 May 2002, Norfolk, VA.
- Burian, S.J., Brown, M.J., and Linger, S.P. (2002b). *Morphological analyses using 3D building databases: Los Angeles, California*. LA-UR-02-0781, Los Alamos National Laboratory, Los Alamos, NM.
- Cionco, R.M. and Ellefsen, R. (1998). "High resolution urban morphology data for urban wind flow modeling." *Atmospheric Environment*, 32(1): 7-17.
- Ellefsen, R. (1990) "Mapping and measuring buildings in the canopy boundary layer in ten U.S. cities." *Energy and Buildings*, 15-16: 1025-1049.
- Grimmond, S. and Oke, T. (1999). "Aerodynamic properties of urban areas derived from analysis of surface form." *J. Appl. Met.*, 38: 1262-1292.
- Hanna, S.R. and Britter, R. (2002). "The effect of roughness obstacles on flow and dispersion in urban industrial areas." *Proceedings, 7th International Conference on Harmonization within Atmospheric Dispersion Modeling for Regulatory Purposes*, Belgirate, Italy, 28-30, May 2002.
- Macdonald, R.W., Griffiths, R.F., and Hall, D.J. (1998). "An improved method for estimation of surface roughness of obstacle arrays." *Atmospheric Environment*, 32: 1857-1864.
- Nichol, J.E. (1996). "High-resolution surface temperature patterns related to urban morphology in a tropical city: A satellite-based study." *J. Appl. Meteor.*, 35: 135-146.
- Oke, T.R. (1988). "Street design and urban canopy layer climate." *Energy and Buildings*, 11: 103-113.
- Ratti, C., Di Sabatino, S., Britter, R., Brown, M., Caton., F., and Burian, S. (2001). "Analysis of 3-D urban databases with respect to pollution dispersion for a number of European and American Cities." *The Third International Conference on Urban Air Quality: Measurement, Modelling, and Management*, March 19-23, 2001, Loutraki, Greece.
-

Raupach, M.R. (1994). "Simplified expressions for vegetation roughness length and zero-plane displacement as functions of canopy height and area index." *Boundary-Layer Meteorology*, 71: 211-216.

Voogt, J. and Oke, T. (1997). "Complete urban surface temperatures." *J. Appl. Met.*, 36: 1117-1132.

Wieringa, J. (1993). "Representative roughness parameters for homogeneous terrain." *Boundary Layer Meteorology*, 63: 323-363.

Appendix 1

Description of Land Use Types

The land use/land cover classification we used for the building analysis was divided into two schemes as shown in Table A1.1. The first scheme corresponds to the Anderson Level 2 classification used by the USGS for its standard national dataset. The second scheme includes the subdivision of the Anderson Level 2 **Residential**, **Commercial & Services**, and **Other Urban or Built-up** categories. Descriptions of the 7-category and 12-category schemes follow Table A1.1. In addition to the multi-level classification we also categorize all the land use parcels that contain high-rise buildings as **Urban High-rise**. Finally, using aerial photographs and other information we defined the downtown city center area and termed this land use as **Downtown Core Area**. Note that **Urban High-rise** and **Downtown Core Area** contain a mix of land use types from Table A1.1.

Table A1.1. The 7-category and 12-category land use classification schemes

Land Use Class
Residential Low-density Single-family (≤ 8 units/hectare) High-density Single-family (> 8 units/hectare) Multifamily Mixed
Commercial & Services Non-high-rise High-rise
Industrial
Transportation/Communications/Utilities
Mixed Industrial & Commercial
Mixed Urban or Built-up
Other Urban or Built-up Predominantly Vegetated Predominantly Built-Up
Urban High-rise
Downtown Core Area

* The 7-category scheme is shown in boldface, the 12-category scheme contains additional categories that are indented

Residential

Includes areas of single-family residences, multi-unit dwellings, mobile homes, and mixtures of residential land use types.

Low-density Single-family: Detached residential housing units with an average density less than or equal to 8 units per hectare (≤ 3 units/acre).

High-density Single-family: Detached residential housing units with an average density greater than 8 units per hectare (> 3 units/acre).

Multifamily: Residential housing units designed to contain multiple families in a single structure. Includes apartments and condominiums.

Mixed: A mixture of low-density single-family, high-density single-family, and multifamily residential land uses.

Commercial & Services

Commercial & Services land use includes areas which are used predominantly for business or the sale of products and their associated services. This category is divided into non-high-rise and high-rise land use types in the 12-category scheme. Includes shopping malls, business districts, office buildings, strip malls, educational and institutional, and other commercial areas.

Industrial

Industrial land use includes areas where manufacturing, assembly, processing, packaging, or storage of products takes place.

Transportation/Communication/Utilities

Areas devoted to major transportation, such as airports, freeways, roads, railways and harbor facilities. Also included are areas devoted to communications and utilities.

Mixed Industrial & Commercial

Areas included are a mixture of industrial and commercial land uses.

Mixed Urban or Built-Up

Areas included are a mixture of the other urban land uses with none being the dominant.

Other Urban or Built-Up

Other land use areas that cannot be categorized in the above categories. Urban vegetation and bare soil classes are categorized in this class for this scheme.

Predominantly Vegetated: Areas included are urban land uses that are predominantly vegetation, such as golf courses, parks, recreation fields, cemeteries, and so on. Some buildings may be contained on the site.

Predominantly Built-up: Includes urban land uses not categorized in any of the above land uses and that are not predominantly vegetated. These land uses are generally ambiguous or unknown.

Urban High-rise

Land use that contains high-rise buildings. High-rise buildings are subjectively selected based on their relative size compared to the surrounding buildings. In general, Urban High-rise was designated for land uses containing buildings with heights in excess of 10 stories.

Downtown Core Area

Subjective designation of the downtown core area based on aerial photograph, street maps, building datasets, and other information.
